Probing redshift-space distortions with phase correlations

Felipe O. Franco,[1] Camille Bonvin,[1] Danail Obreschkow,[2,3] Kamran Ali,[2,3] and Joyce Byun[1]

[1]*Département de Physique Théorique and Center for Astroparticle Physics (CAP),*
University of Geneva, 24 quai Ernest Ansermet, CH-1211 Geneva, Switzerland
[2]*International Centre for Radio Astronomy Research (ICRAR), University of Western Australia,*
35 Stirling Highway, Crawley Western Australia 6009, Australia
[3]*ARC Centre of Excellence for All-sky Astrophysics (CAASTRO)*

Redshift-space distortions are a sensitive probe of the growth of large-scale structure. In the linear regime, redshift-space distortions are fully described by the multipoles of the two-point correlation function. In the nonlinear regime, however, higher-order statistics are needed to capture the full information of the galaxy density field. In this paper, we show that the redshift-space line correlation function—which is a measure of Fourier phase correlations—is sensitive to the nonlinear growth of the density and velocity fields and to the nonlinear mapping between real and redshift space. We expand the line correlation function in multipoles, and we show that almost all of the information is encoded in the monopole, quadrupole, and hexadecapole. We argue that these multipoles are highly complementary to the multipoles of the two-point correlation function: first, because they are directly sensitive to the difference between the density and the velocity coupling kernels, which is a purely nonlinear quantity; and second, because the multipoles are proportional to different combinations of f and σ_8. Measured in conjunction with the two-point correlation function and the bispectrum, the multipoles of the line correlation function could therefore allow us to disentangle efficiently these two quantities and to test modified theories of gravity.

I. INTRODUCTION

Cosmological galaxy redshift surveys, like the 6dF Galaxy Redshift Survey [1], Sloan Digital Sky Survey [2], WiggleZ survey [3], VIPERS survey [4], or BOSS survey [5], map the distribution of galaxies in redshift space. Since the redshift of galaxies is affected by their peculiar velocity, the observed galaxy distribution is slightly distorted with respect to the real-space galaxy distribution. In the linear regime, these redshift-space distortions modify the two-point correlation function and the power spectrum, by adding a quadrupole and an hexadecapole modulation in the signal [6,7]. Measuring these multipoles has been one of the main goals of recent redshift galaxy surveys; see, e.g., [8]. These measurements have been very successful and have provided constraints on modified theories of gravity [9]. Redshift-space distortions are indeed highly sensitive to the growth rate of perturbation f, which is generally modified in alternative theories of gravity.

In the nonlinear regime, the multipoles of the correlation function do however not fully trace the information present in galaxy surveys. The nonlinear gravitational evolution of the density and peculiar velocity generates indeed a flow of information into higher-order statistics. An obvious choice to capture this flow of information is to look at the three-point correlation function (or Fourier-space bispectrum); see, e.g., [10–12] and Refs. therein. However, this estimator is a three-dimensional function with significant redundancies with itself and the two-point statistics, making its computation and information analysis a complex task.

Various alternative observables have been constructed in order to access information in the nonlinear regime; see, e.g., [13–16]. The goal of such observables is twofold: first, part of the information present in the bispectrum has already been measured in the power spectrum. One can then wonder if it is possible to construct an observable which is less redundant with the power spectrum. And second, since the bispectrum is complicated in redshift space, it would be interesting to construct an estimator which encodes the same type of information, but which is simpler to model.

In this paper, we study one possible alternative: the line correlation function. The line correlation function has been introduced in [17] and analytically modeled in real space in [18]. This observable is constructed from correlations between the *phases* of the density field. Since the two-point function is only sensitive to the *amplitude* of the density field, it seems promising to use in conjunction an observable which is targeted to measure the phases (see [19–33] for other observables based on phase correlations). Fisher forecasts in real space have shown that combining the line correlation function with the two-point correlation function does indeed improve parameter constraints on ΛCDM cosmology by up to a factor of 2 [34,35]. The gain

obtained from the line correlation function in the case of a warm dark matter model or alternative theories of gravity, like the symmetron and $f(R)$ model is even stronger [36].

Here we derive an expression for the line correlation function in redshift space. We show that the line correlation function can be expanded in Legendre polynomials and that almost all of the information is encoded in the first even three multipoles, i.e., the monopole, quadrupole, and hexadecapole, similarly to the two-point correlation function. These multipoles are sensitive to the nonlinear coupling kernels of the density and of the peculiar velocity. As such, the line correlation function provides a simple way to probe the nonlinear evolution in redshift space and consequently, to constrain alternative theories of gravity in the nonlinear regime, for example, at the scales where screening mechanisms start to act. Note that our approach differs and complements the work of [37], which studies a modified version of the line correlation function (using an anisotropic window function) and is targeted to measure an anisotropic signal in two-dimensional Zel'dovich mock density fields.

Let us mention that throughout this paper we will use second-order perturbation theory to model redshift-space distortions. Studies of the bispectrum have shown that this approach does not fully account for nonlinearities in redshift space. Various models have been developed over the years to provide a more accurate description of redshift-space distortions, either by improving on perturbation theory [10,38,39] or by building effective coupling kernels based on numerical simulations [12]. In particular, these models are able to describe the Fingers of God, which are not accounted for at second order in perturbation theory. However, since it is not clear which of these models is more adapted to describe phase correlations, we start by using only second-order perturbation theory. Our modeling should therefore be regarded as a first step towards an accurate description of phase correlations in redshift space. In a future work, we will compare our modeling with measurements of the line correlation function in numerical simulations, in order to improve the description of redshift-space distortions in the strongly nonlinear regime.

The remainder of the paper is organized as follows. In Sec. II, we derive an expression for the line correlation function in redshift space, at second order in perturbation theory. In Sec. III, we expand the line correlation function in Legendre polynomials. We derive a general expression valid for any multipole n. In Sec. IV, we calculate numerically the first multipoles in a ΛCDM universe, and we show that the multipoles larger than $n = 4$ are negligible. We conclude in Sec. V.

II. THE LINE CORRELATION FUNCTION OF THE OBSERVED NUMBER COUNTS

Galaxy surveys measure the overdensity of galaxies in redshift space,

$$\Delta(\mathbf{n}, z) = \frac{N(\mathbf{n}, z) - \bar{N}(z)}{\bar{N}(z)}, \quad (1)$$

where $N(\mathbf{n}, z)$ denotes the number of galaxies detected in a pixel situated at redshift z and in direction $\mathbf{n}$, and $\bar{N}(z)$ is the average number of galaxies per pixel at a given redshift. The Fourier transform of the galaxy overdensity,[1] $\Delta(\mathbf{k}, z)$, is characterized by an amplitude $|\Delta(\mathbf{k}, z)|$ and a phase

$$\epsilon_\Delta(\mathbf{k}, z) \equiv \frac{\Delta(\mathbf{k}, z)}{|\Delta(\mathbf{k}, z)|}. \quad (2)$$

The line correlation function of Δ is then defined as

$$\ell(\mathbf{r}, z) = \frac{V^3}{(2\pi)^9} \left(\frac{r^3}{V}\right)^{3/2} \langle \epsilon_\Delta(\mathbf{s}, z) \epsilon_\Delta(\mathbf{s}+\mathbf{r}, z) \epsilon_\Delta(\mathbf{s}-\mathbf{r}, z) \rangle$$

$$= \frac{V^3}{(2\pi)^9} \left(\frac{r^3}{V}\right)^{3/2} \int \underset{\substack{|\mathbf{k}_1|,|\mathbf{k}_2|, \\ |\mathbf{k}_3| \leq 2\pi/r}}{\int \int} d^3\mathbf{k}_1 d^3\mathbf{k}_2 d^3\mathbf{k}_3 e^{i(\mathbf{k}_1+\mathbf{k}_2+\mathbf{k}_3)\cdot\mathbf{s}}$$

$$\times e^{i(\mathbf{k}_2-\mathbf{k}_3)\cdot\mathbf{r}} \langle \epsilon_\Delta(\mathbf{k}_1, z) \epsilon_\Delta(\mathbf{k}_2, z) \epsilon_\Delta(\mathbf{k}_3, z) \rangle, \quad (3)$$

where $\epsilon_\Delta(\mathbf{s}, z)$ is the inverse Fourier transform of $\epsilon_\Delta(\mathbf{k}, z)$. As discussed in [17], the cutoff at high k has been introduced to avoid the divergence of the line correlation function due to an infinite number of phase factors at arbitrarily small scales, which do not carry any information.

We start by calculating the three-point correlation function of the phase of $\Delta(\mathbf{k}, z)$. For this, we need a description of the galaxy number count valid at second order in perturbation theory. At first order in perturbation theory, we have the standard Kaiser expression,

$$\Delta^{(1)}(\mathbf{n}, z) = b_1 \delta^{(1)} - \frac{1}{\mathcal{H}} \partial_\chi(\mathbf{v}^{(1)} \cdot \mathbf{n}), \quad (4)$$

where $\mathcal{H} = (da/d\eta)/a$ is the Hubble parameter in conformal time η, b_1 is the linear bias, δ is the matter density field, $\mathbf{v}$ is the peculiar velocity of galaxy, and ∂_χ denotes radial derivative (χ being the conformal distance). The second term in Eq. (4) represents the contribution from redshift-space distortions. Note that Δ contains various other contributions, namely relativistic effects and lensing effects [40–42], but we neglect these terms here since we are mainly interested in small scales and low redshifts, where they are expected to be subdominant.

At second order in perturbation theory, we can identify two types of contributions: first, the contribution coming from the nonlinear gravitational evolution of the density and peculiar velocity field. We call this contribution the *intrinsic* contribution, $\Delta_{\text{int}}^{(2)}$, because it is due to the fact that

---

[1]We use the Fourier convention $f(\mathbf{x}) = \int d^3\mathbf{k}\, e^{i\mathbf{x}\cdot\mathbf{k}} f(\mathbf{k})$ and $f(\mathbf{k}) = \int \frac{d^3\mathbf{x}}{(2\pi)^3} e^{-i\mathbf{x}\cdot\mathbf{k}} f(\mathbf{x})$.

the density, velocity, and bias are intrinsically nonlinear quantities,

$$\Delta_{\text{int}}^{(2)}(\mathbf{n}, z) = b_1 \delta^{(2)} - \frac{1}{\mathcal{H}} \partial_\chi (\mathbf{v}^{(2)} \cdot \mathbf{n})$$
$$+ \frac{b_2}{2} [(\delta^{(1)})^2 - \langle (\delta^{(1)})^2 \rangle] + \frac{b_{s^2}}{2} [s^2 - \langle s^2 \rangle], \quad (5)$$

where s denotes the tidal tensor [43].

In addition, at second order, we have contributions coming from the fact that the mapping between real space and redshift space is itself nonlinear. We call these contributions $\Delta_{\text{map}}^{(2)}$. A detailed derivation is given in Appendix A, following [44]. The result is

$$\Delta_{\text{map}}^{(2)}(\mathbf{n}, z) = -\frac{b_1}{\mathcal{H}} \delta^{(1)} \partial_\chi (\mathbf{v}^{(1)} \cdot \mathbf{n}) - \frac{b_1}{\mathcal{H}} \partial_\chi \delta^{(1)} (\mathbf{v}^{(1)} \cdot \mathbf{n})$$
$$+ \frac{1}{\mathcal{H}^2} \partial_\chi [\partial_\chi (\mathbf{v}^{(1)} \cdot \mathbf{n})(\mathbf{v}^{(1)} \cdot \mathbf{n})]. \quad (6)$$

Note that besides these dominant contributions, many other terms contribute to Δ_{map} at second order, due to lensing and relativistic effects [45–47]. But again we neglect them here since they are expected to become relevant on larger scales and higher redshifts.

Since Δ is expressed in terms of the observed coordinates $\mathbf{x}_{\text{obs}} = \chi(z)\mathbf{n}$, where χ is the comoving distance evaluated at the observed redshift z, we can consistently Fourier transform it,

$$\Delta(\mathbf{k}, z) = \frac{1}{(2\pi)^3} \int d^3 \mathbf{x}_{\text{obs}} e^{-i\mathbf{k} \cdot \mathbf{x}_{\text{obs}}} \Delta(\mathbf{x}_{\text{obs}}, z). \quad (7)$$

At first order in perturbation theory, we obtain

$$\Delta^{(1)}(\mathbf{k}, z) = b_1 \delta^{(1)}(\mathbf{k}, z) - \frac{1}{\mathcal{H}} (\hat{\mathbf{k}} \cdot \mathbf{n})^2 V^{(1)}(\mathbf{k}, z),$$
$$= (b_1 + f\mu^2) \delta^{(1)}(\mathbf{k}, z), \quad (8)$$

where V is related to the Fourier transform of $\mathbf{v}$ by

$$\mathbf{v}(\mathbf{k}, z) = -i \frac{\hat{\mathbf{k}}}{k} V(\mathbf{k}, z) \quad (9)$$

and $\mu = \hat{\mathbf{k}} \cdot \mathbf{n}$. In the second line of (8), we have used the continuity equation at linear order to relate the velocity to the density, and we define the growth rate as

$$f = \frac{d \ln D_1}{d \ln a}, \quad (10)$$

where D_1 is the linear growth function.

At second order in perturbation theory, the density field $\delta^{(2)}$ and the velocity field $V^{(2)}$ take the form,

$$\delta^{(2)}(\mathbf{k}, z) = \int d^3 \mathbf{q}_1 \int d^3 \mathbf{q}_2 \delta_D(\mathbf{k} - \mathbf{q}_1 - \mathbf{q}_2)$$
$$\times F_2(\mathbf{q}_1, \mathbf{q}_2) \delta^{(1)}(\mathbf{q}_1, z) \delta^{(1)}(\mathbf{q}_2, z), \quad (11)$$

$$V^{(2)}(\mathbf{k}, z) = -\mathcal{H}(z) f(z) \int d^3 \mathbf{q}_1 \int d^3 \mathbf{q}_2 \delta_D(\mathbf{k} - \mathbf{q}_1 - \mathbf{q}_2)$$
$$\times G_2(\mathbf{q}_1, \mathbf{q}_2) \delta^{(1)}(\mathbf{q}_1, z) \delta^{(1)}(\mathbf{q}_2, z), \quad (12)$$

where the nonlinear kernels are given by [48,49]

$$F_2(\mathbf{k}_1, \mathbf{k}_2) = \frac{1 + \epsilon_F}{2} + \frac{\hat{\mathbf{k}}_1 \cdot \hat{\mathbf{k}}_2}{2} \left(\frac{k_1}{k_2} + \frac{k_2}{k_1} \right)$$
$$+ \frac{1 - \epsilon_F}{2} (\hat{\mathbf{k}}_1 \cdot \hat{\mathbf{k}}_2)^2, \quad (13)$$

$$G_2(\mathbf{k}_1, \mathbf{k}_2) = \epsilon_G + \frac{\hat{\mathbf{k}}_1 \cdot \hat{\mathbf{k}}_2}{2} \left(\frac{k_1}{k_2} + \frac{k_2}{k_1} \right)$$
$$+ (1 - \epsilon_G)(\hat{\mathbf{k}}_1 \cdot \hat{\mathbf{k}}_2)^2, \quad (14)$$

with $\epsilon_F \simeq (3/7)\Omega_m(z)^{-1/143}$ and $\epsilon_G = \epsilon_F + (3/2)(\epsilon_F - 3/7)$. The kernels depend therefore very mildly on z through ϵ_F and ϵ_G.

With this, the intrinsic part becomes at second order

$$\Delta_{\text{int}}^{(2)}(\mathbf{k}, z) = \int d^3 \mathbf{q}_1 \int d^3 \mathbf{q}_2 \delta_D(\mathbf{k} - \mathbf{q}_1 - \mathbf{q}_2)$$
$$\times \left[b_1 F_2(\mathbf{q}_1, \mathbf{q}_2) + \frac{b_2}{2} + \frac{b_{s^2}}{2} S_2(\mathbf{q}_1, \mathbf{q}_2) \right.$$
$$\left. + f\mu^2 G_2(\mathbf{q}_1, \mathbf{q}_2) \right] \delta^{(1)}(\mathbf{q}_1, z) \delta^{(1)}(\mathbf{q}_2, z), \quad (15)$$

where $\mu = \hat{\mathbf{k}} \cdot \mathbf{n}$ and $S_2(\mathbf{q}_1, \mathbf{q}_2) = (\hat{\mathbf{q}}_1 \cdot \hat{\mathbf{q}}_2)^2 - 1/3$.

Finally, the mapping part at second order can be written as

$$\Delta_{\text{map}}^{(2)}(\mathbf{k}, z) = \int d^3 \mathbf{q}_1 \int d^3 \mathbf{q}_2 \delta_D(\mathbf{k} - \mathbf{q}_1 - \mathbf{q}_2)$$
$$\times \frac{f\mu k}{2} \left[\frac{\mu_1}{q_1} (b_1 + f\mu_2^2) + \frac{\mu_2}{q_2} (b_1 + f\mu_1^2) \right]$$
$$\times \delta^{(1)}(\mathbf{q}_1, z) \delta^{(1)}(\mathbf{q}_2, z), \quad (16)$$

where $\mu_i = \hat{\mathbf{q}}_i \cdot \mathbf{n}$, $i = 1, 2$. Note that the mapping term is often computed in a different way. Instead of writing Δ as a function of the observed coordinate $\mathbf{x}_{\text{obs}}$ as we did here and then Fourier transform it, one can express Δ in terms of the unperturbed coordinate $\mathbf{x}$ and then expand the exponential in the Fourier transform around $\mathbf{x}$ (see Appendix A for more detail). This procedure gives rise to the same expression for $\Delta_{\text{map}}^{(2)}(\mathbf{k}, z)$. Note that this term is sometimes defined as part of the Finger of God contribution, since it arises from the exponential in the Fourier transform. We reserve however this name for the damping due to the random motion of galaxies at small scales (see, e.g., [10,50]), which we do not include in our derivation, since it is not captured by second-order perturbation theory.

We now compute the three-point correlation function of the phase of $\Delta(\mathbf{k}, z)$, which enters in Eq. (3). We have

$$\langle \epsilon_\Delta(\mathbf{k}_1)\epsilon_\Delta(\mathbf{k}_2)\epsilon_\Delta(\mathbf{k}_3)\rangle = \int [d\theta]\mathcal{P}[\theta]\epsilon_\Delta(\mathbf{k}_1)\epsilon_\Delta(\mathbf{k}_2)\epsilon_\Delta(\mathbf{k}_3),$$
(17)

where $\mathcal{P}[\theta]$ is the probability distribution function of the field $\theta(\mathbf{k})$ defined through $\epsilon_\Delta(\mathbf{k}) = e^{i\theta(\mathbf{k})}$. Note that here we have dropped the dependence in redshift z in the argument of ϵ_Δ to ease the notation. Following [18,30], we start by expressing the probability distribution function for $\Delta(\mathbf{k}, z)$ using the Edgeworth expansion [51–53], which is valid for mildly non-Gaussian fields,

$$\mathcal{P}[\Delta] = N_G \exp\left(-\frac{1}{2}\int d^3\mathbf{k}\frac{\Delta(\mathbf{k})\Delta(-\mathbf{k})}{P_\Delta(\mathbf{k})}\right)\left\{1 + \frac{1}{3!}\int d^3\mathbf{p}d^3\mathbf{q}\frac{B_\Delta(\mathbf{p},\mathbf{q},-\mathbf{p}-\mathbf{q})\Delta(-\mathbf{p})\Delta(-\mathbf{q})\Delta(\mathbf{p}+\mathbf{q})}{P_\Delta(\mathbf{p})P_\Delta(\mathbf{q})P_\Delta(\mathbf{p}+\mathbf{q})}\right\}, \quad (18)$$

where N_G is a normalization factor. Here, $P_\Delta(\mathbf{k})$ and $B_\Delta(\mathbf{p},\mathbf{q},\mathbf{k})$ are the power spectrum and bispectrum of Δ defined through

$$\langle \Delta(\mathbf{k})\Delta(\mathbf{k}')\rangle = P_\Delta(\mathbf{k})\delta_D(\mathbf{k}+\mathbf{k}'),$$
(19)

$$\langle \Delta(\mathbf{p})\Delta(\mathbf{q})\Delta(\mathbf{k})\rangle = B_\Delta(\mathbf{p},\mathbf{q})\delta_D(\mathbf{p}+\mathbf{q}+\mathbf{k}).$$
(20)

Note that since redshift-space distortions break statistical isotropy, $P_\Delta(\mathbf{k})$ depends not only on the modulus of $\mathbf{k}$ but also on its orientation with respect to the direction of observation $\mathbf{n}$. Similarly, the bispectrum depends not only on the shape of the triangle but also on its orientation.

Following the derivation in [18], we first discretize the field $\Delta(\mathbf{k}) \to \Delta_\mathbf{k}$ for a finite survey volume, and then we integrate over the amplitude $|\Delta_\mathbf{k}|$ to obtain the probability distribution function of the phase,

$$\mathcal{P}(\{\theta_\mathbf{k}\})\prod_{\mathbf{k}\in\text{uhs}} d\theta_\mathbf{k} = \left\{1 + \frac{\sqrt{\pi}}{6}\sum_{\mathbf{p}\in\text{uhs}} b_\Delta(\mathbf{p},\mathbf{p})\cos(2\theta_\mathbf{p} - \theta_{2\mathbf{p}}) + \frac{1}{3}\left(\frac{\sqrt{\pi}}{2}\right)^3\sum_{\mathbf{p}\neq\mathbf{q}\in\text{uhs}}[b_\Delta(\mathbf{p},\mathbf{q})\cos(\theta_\mathbf{p} + \theta_\mathbf{q} - \theta_{\mathbf{p}+\mathbf{q}})\right.$$
$$\left. + b_\Delta(\mathbf{p},-\mathbf{q})\cos(\theta_\mathbf{p} - \theta_\mathbf{q} + \theta_{\mathbf{p}-\mathbf{q}})]\right\}\prod_{\mathbf{k}\in\text{uhs}}\frac{d\theta_\mathbf{k}}{2\pi}, \quad (21)$$

where we have defined

$$b_\Delta(\mathbf{p},\mathbf{q}) \equiv \sqrt{\frac{(2\pi)^3}{V}}\frac{B_\Delta(\mathbf{p},\mathbf{q})}{\sqrt{P_\Delta(\mathbf{p})P_\Delta(\mathbf{q})P_\Delta(\mathbf{k})}}.$$
(22)

Inserting Eq. (21) into (17), we obtain in the continuous limit,

$$\langle \epsilon_\Delta(\mathbf{k}_1)\epsilon_\Delta(\mathbf{k}_2)\epsilon_\Delta(\mathbf{k}_3)\rangle = \frac{(2\pi)^3}{V}\left(\frac{\sqrt{\pi}}{2}\right)^3 b_\Delta(\mathbf{k}_1,\mathbf{k}_2,\mathbf{k}_3)\delta_D(\mathbf{k}_1+\mathbf{k}_2+\mathbf{k}_3).$$
(23)

At second order in perturbation theory, we have

$$b_\Delta(\mathbf{k}_1,\mathbf{k}_2,\mathbf{k}_3) = 2\sqrt{\frac{(2\pi)^3}{V}}\left[W_2(\mathbf{k}_1,\mathbf{k}_2,\mathbf{k}_3,\mathbf{n})\sqrt{\frac{P_L(k_1,z)P_L(k_2,z)}{P_L(k_3,z)}} + \text{cyc}\right],$$
(24)

where P_L denotes the linear power spectrum of δ at redshift z and

$$W_2(\mathbf{k}_1,\mathbf{k}_2,\mathbf{k}_3,\mathbf{n}) = W_2^{\text{int}}(\mathbf{k}_1,\mathbf{k}_2,\mathbf{k}_3,\mathbf{n}) + W_2^{\text{map}}(\mathbf{k}_1,\mathbf{k}_2,\mathbf{k}_3,\mathbf{n}).$$
(25)

The intrinsic and mapping kernels read

$$W_2^{\text{int}} = \frac{1}{b_1 + \mu_3^2 f}\times\left[b_1 F_2(\mathbf{k}_1,\mathbf{k}_2) + \frac{b_2}{2} + \frac{b_{s^2}}{2}S_2(\mathbf{k}_1,\mathbf{k}_2) + \mu_3^2 f G_2(\mathbf{k}_1,\mathbf{k}_2)\right],$$
(26)

$$W_2^{\mathrm{map}} = -\frac{f\mu_3 k_3[\frac{\mu_1}{k_1}(b_1 + f\mu_2^2) + \frac{\mu_2}{k_2}(b_1 + f\mu_1^2)]}{2(b_1 + \mu_3^2 f)}, \quad (27)$$

with $\mu_i = \hat{\mathbf{k}}_i \cdot \mathbf{n}$ for $i = 1, 2, 3$.

We see that the phase correlation of the observed number count Δ is sensitive to the nonlinear coupling kernel of the density field F_2, to the nonlinear coupling kernel of the velocity field G_2, and to the growth rate f. Since redshift-space distortions are not isotropic, the phase correlations depend on the direction of observation $\mathbf{n}$. Note that here we work in the distant-observer approximation, where $\mathbf{n}$ is the same for all galaxies.

The line correlation function is obtained by inserting (24) and (23) into (3). We get

$$\ell(\mathbf{r}, z) = \frac{r^{9/2}}{8\sqrt{2}(2\pi)^3} \int\int_{\substack{|\mathbf{k}_1|,|\mathbf{k}_2|,\\ |\mathbf{k}_1+\mathbf{k}_2|\le 2\pi/r}} d^3\mathbf{k}_1 d^3\mathbf{k}_2 W_2(-\mathbf{k}_1 - \mathbf{k}_2, \mathbf{k}_1, \mathbf{k}_2, \mathbf{n})\sqrt{\frac{P_L(|\mathbf{k}_1 + \mathbf{k}_2|, z)P_L(k_1, z)}{P_L(k_2, z)}}$$
$$\times [e^{i(\mathbf{k}_1 - \mathbf{k}_2)\cdot\mathbf{r}} + e^{i(\mathbf{k}_1 + 2\mathbf{k}_2)\cdot\mathbf{r}} + e^{-i(2\mathbf{k}_1 + \mathbf{k}_2)\cdot\mathbf{r}}]. \quad (28)$$

Here, we have used the Dirac Delta function to rewrite the three permutations in (24) with the same kernel W_2 multiplied by three different exponentials. In this way, the kernel W_2 depends on the direction of observation $\mathbf{n}$ only through its scalar product with $\mathbf{k}_2$. We will see that this property is useful to solve analytically some of the integrals in (28).

Since redshift-space distortions break isotropy, the line correlation function depends not only on the modulus of the separation $r = |\mathbf{r}|$, but also on the orientation of the vector $\mathbf{r}$ with respect to the line-of-sight: $\cos\alpha = \hat{\mathbf{r}} \cdot \mathbf{n}$, as depicted in Fig. 1. In the rest of this paper, we will study the dependence of the line correlation function on α. Note that in the case where $f = 0$, Eq. (28) is equivalent to the expression derived in [18].

III. MULTIPOLE EXPANSION OF THE LINE CORRELATION FUNCTION

In redshift space, the two-point correlation function of Δ can be written as the sum of a monopole, quadrupole, and
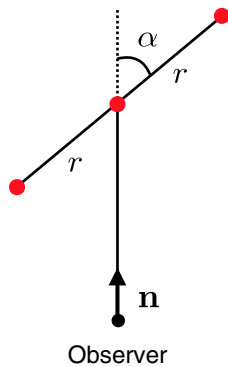

FIG. 1. Representation of the coordinate system used to express the line correlation function: $r = |\mathbf{r}|$ denotes the separation between galaxies, and $\cos\alpha = \hat{\mathbf{r}} \cdot \mathbf{n}$ is the orientation of the line with respect to the direction of observation $\mathbf{n}$. We work in the distant-observer approximation, in which $\mathbf{n}$ is the same for all galaxies.

hexadecapole in the angle α. At linear order in perturbation theory and using the distant-observer approximation, one can show that these three multipoles encode all the information present in the two-point correlation function [7].

Contrary to the two-point correlation function, the line correlation function cannot be simply expressed as a sum of the first three even Legendre polynomials only. However, we will see that the contribution from the multipoles larger than $n = 4$ is actually negligible so that most of the information about redshift-space distortions is indeed encoded in the monopole, quadrupole, and hexadecapole of ℓ.

Since the Legendre polynomials form a basis, we can expand the line correlation function as

$$\ell(r, \alpha, z) = \sum_{n=0}^{\infty} Q_n(r, z)L_n(\cos\alpha), \quad (29)$$

where $\cos\alpha = \hat{\mathbf{r}} \cdot \mathbf{n}$ and L_n denotes the Legendre polynomial of order n. The multipole of order n can be measured by weighting the line correlation function by the appropriate Legendre polynomial,

$$Q_n(r, z) = \frac{2n + 1}{2} \int_{-1}^{1} d\mu\, \ell(r, \mu, z)L_n(\mu), \quad (30)$$

where $\mu = \cos\alpha$.

To calculate explicitly Q_n, we insert Eq. (28) into (29) and we expand the exponentials in (28) and the Legendre polynomial in (29) in terms of spherical harmonics,

$$e^{i\mathbf{k}\cdot\mathbf{r}} = 4\pi \sum_{n=0}^{\infty} \sum_{m=-n}^{n} i^n j_n(kr)Y_{nm}^*(\hat{\mathbf{k}})Y_{nm}(\hat{\mathbf{r}}), \quad (31)$$

$$L_n(\mu) = \frac{4\pi}{2n + 1} \sum_{m=-n}^{n} Y_{nm}(\mathbf{n})Y_{nm}^*(\hat{\mathbf{r}}). \quad (32)$$

We obtain

$$Q_n(r,z) = \frac{r^{9/2}}{8\sqrt{2}(2\pi)^3} 8\pi^2 \sum_{m=-n}^{n} \sum_{n'=0}^{\infty} \sum_{m'=-n'}^{n'} i^{n'} \int_{-1}^{1} d\mu \, Y_{nm}^*(\hat{\mathbf{r}}) Y_{n'm'}(\hat{\mathbf{r}}) Y_{nm}(\mathbf{n}) \iint_{\substack{|\mathbf{k}_1|,|\mathbf{k}_2|, \\ |\mathbf{k}_1+\mathbf{k}_2|\leq 2\pi/r}} d^3\mathbf{k}_1 d^3\mathbf{k}_2$$

$$\times W_2(-\mathbf{k}_1 - \mathbf{k}_2, \mathbf{k}_1, \mathbf{k}_2, \mathbf{n}) \sqrt{\frac{P_L(|\mathbf{k}_1+\mathbf{k}_2|,z)P_L(k_1,z)}{P_L(k_2,z)}} [j_{n'}(\kappa_1 r) Y_{n'm'}^*(\hat{\boldsymbol{\kappa}}_1) + j_{n'}(\kappa_2 r) Y_{n'm'}^*(\hat{\boldsymbol{\kappa}}_2) + j_{n'}(\kappa_3 r) Y_{n'm'}^*(\hat{\boldsymbol{\kappa}}_3)],$$

$$\tag{33}$$

where

$$\boldsymbol{\kappa}_1 \equiv \mathbf{k}_1 - \mathbf{k}_2, \tag{34}$$

$$\boldsymbol{\kappa}_2 \equiv \mathbf{k}_1 + 2\mathbf{k}_2, \tag{35}$$

$$\boldsymbol{\kappa}_3 \equiv -2\mathbf{k}_1 - \mathbf{k}_2. \tag{36}$$

Since in the distant-observer approximation, the direction of observation $\mathbf{n}$ is fixed for all galaxies, we can choose $\mathbf{n}$ on the $\hat{\mathbf{z}}$ axis without loss of generality. The integral over μ in Eq. (33) becomes then an integral over the direction of $\mathbf{r}$, which can be performed and gives rise to $\delta_{nn'}\delta_{mm'}$. Combining the remaining spherical harmonics into Legendre polynomials, we obtain

$$Q_n(r,z) = \frac{r^{9/2}(2n+1)}{8\sqrt{2}(2\pi)^3} i^n \iint_{\substack{|\mathbf{k}_1|,|\mathbf{k}_2|, \\ |\mathbf{k}_1+\mathbf{k}_2|\leq 2\pi/r}} d^3\mathbf{k}_1 d^3\mathbf{k}_2 W_2(-\mathbf{k}_1-\mathbf{k}_2, \mathbf{k}_1, \mathbf{k}_2, \mathbf{n}) \sqrt{\frac{P_L(|\mathbf{k}_1+\mathbf{k}_2|,z)P_L(k_1,z)}{P_L(k_2,z)}}$$

$$\times [j_n(\kappa_1 r)L_n(\hat{\boldsymbol{\kappa}}_1 \cdot \mathbf{n}) + j_n(\kappa_2 r)L_n(\hat{\boldsymbol{\kappa}}_2 \cdot \mathbf{n}) + j_n(\kappa_3 r)L_n(\hat{\boldsymbol{\kappa}}_3 \cdot \mathbf{n})]. \tag{37}$$

Equation (37) contains a six-dimensional integral. We now show how to reduce it to a three-dimensional integral that we can compute numerically.

A. Multipoles due to the intrinsic contribution

We start by calculating the multipoles generated by the intrinsic kernel (26). Let us denote by (θ_1, ϕ_1) and (θ_2, ϕ_2) the angular coordinates of $\mathbf{k}_1$ and $\mathbf{k}_2$. Since we have fixed the direction of observation $\mathbf{n}$ on the $\hat{\mathbf{z}}$ axis, we have $\hat{\mathbf{k}}_2 \cdot \mathbf{n} = \cos\theta_2$. We first do a change of variables from $\{\theta_1, \phi_1, \theta_2, \phi_2\} \rightarrow \{\gamma, \varphi, \theta_2, \phi_2\}$, where $\cos\gamma = \hat{\mathbf{k}}_1 \cdot \hat{\mathbf{k}}_2$ and φ is the azimuthal angle of $\mathbf{k}_1$ around $\mathbf{k}_2$; see Fig. 2. The Jacobian of this transformation is 1, since it is a rotation. In Eq. (37), the only quantities that depend on φ and ϕ_2 are the Legendre polynomials. We have

$$\hat{\boldsymbol{\kappa}}_1 \cdot \mathbf{n} = \frac{-k_1\sin\gamma\sin\theta_2\cos(\varphi-\phi_2)+(k_1\cos\gamma-k_2)\cos\theta_2}{\sqrt{k_1^2+k_2^2-2k_1k_2\cos\gamma}},$$

$$\hat{\boldsymbol{\kappa}}_2 \cdot \mathbf{n} = \frac{-k_1\sin\gamma\sin\theta_2\cos(\varphi-\phi_2)+(k_1\cos\gamma+2k_2)\cos\theta_2}{\sqrt{k_1^2+4k_2^2+4k_1k_2\cos\gamma}},$$

$$\hat{\boldsymbol{\kappa}}_3 \cdot \mathbf{n} = \frac{2k_1\sin\gamma\sin\theta_2\cos(\varphi-\phi_2)-(2k_1\cos\gamma+k_2)\cos\theta_2}{\sqrt{4k_1^2+k_2^2+4k_1k_2\cos\gamma}}.$$

For any value of n, the integral over ϕ_2 and φ can be done analytically, since the Legendre polynomials can always be

expressed as a series of cosines. For odd n's, we find that the integrals vanish, as expected due to the symmetry of the line correlation function. We present here the derivation and explicit expression for the monopole $n = 0$, the quadrupole $n = 2$ and the hexadecapole $n = 4$. In Appendix B, we derive a general expression valid for any n.

1. The monopole of the intrinsic contribution

For the monopole, the integral over ϕ_2 and φ in Eq. (37) trivially gives $4\pi^2$ since the Legendre polynomials are constant. The integral over θ_2 can then be performed analytically

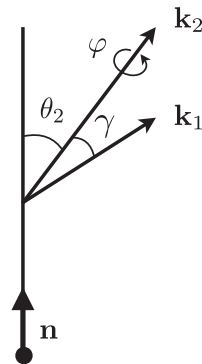FIG. 2. Definition of the angles θ_2, γ, and φ used in the calculation of the multipoles Q_n.

$$\int_{-1}^{1} d\mu_2 \frac{b_1 F_2 + b_2/2 + b_{s^2} S_2/2 + \mu_2^2 f G_2}{b_1 + \mu_2^2 f} = 2 \left[G_2 + \left(F_2 - G_2 + \frac{b_2}{2b_1} + \frac{b_{s^2}}{2b_1} S_2 \right) \frac{\arctan \sqrt{\beta}}{\sqrt{\beta}} \right], \tag{38}$$

where $\mu_2 = \cos \theta_2$ and

$$\beta \equiv \frac{f}{b_1}. \tag{39}$$

The monopole then simply becomes

$$Q_0^{\text{int}}(r,z) = \frac{r^{9/2}}{8\pi\sqrt{2}} \int_0^{2\pi/r} dk_1 k_1^2 \int_0^{2\pi/r} dk_2 k_2^2 \int_{-1}^{\nu_{\text{cut}}} d\nu \sqrt{\frac{P_L(|\mathbf{k}_1 + \mathbf{k}_2|, z) P_L(k_1, z)}{P_L(k_2, z)}} \bigg\{ F_2(-\mathbf{k}_1 - \mathbf{k}_2, \mathbf{k}_1)$$
$$+ \left(\frac{b_2}{2b_1} + \frac{b_{s^2}}{2b_1} S_2(-\mathbf{k}_1 - \mathbf{k}_2, \mathbf{k}_1) \right) \frac{\arctan \sqrt{\beta}}{\sqrt{\beta}} + (F_2 - G_2)(-\mathbf{k}_1 - \mathbf{k}_2, \mathbf{k}_1) \left(\frac{\arctan \sqrt{\beta}}{\sqrt{\beta}} - 1 \right) \bigg\} \sum_{i=1}^{3} j_0(\kappa_i r), \tag{40}$$

where

$$\nu_{\text{cut}} = \min\{1, \max\{-1, [(2\pi/r)^2 - k_1^2 - k_2^2]/[2k_1 k_2]\}\}$$

enforces the condition $|\mathbf{k}_1 + \mathbf{k}_2| \le 2\pi/r$. Here, the kernel F_2 and G_2, and the κ_i defined in Eqs. (34)–(36) can be expressed as functions of k_1, k_2 and $\nu = \cos \gamma = \hat{\mathbf{k}}_1 \cdot \hat{\mathbf{k}}_2$ only. Equation (40) contains three integrals that can be computed numerically.

2. The quadrupole of the intrinsic contribution

To calculate the quadrupole, we first need to integrate the terms in the square bracket in Eq. (37) over ϕ_2 and φ. As an example, let us look at the first term. We have

$$\int_0^{2\pi} d\phi_2 \int_0^{2\pi} d\varphi L_2(\hat{\kappa}_1 \cdot \mathbf{n}) = (2\pi)^2 \left[1 - \frac{3}{2} \frac{k_1^2 (1 - \nu^2)}{\kappa_1^2} \right] L_2(\cos \theta_2). \tag{41}$$

As for the monopole, the integral over θ_2 can then be performed analytically

$$\int_{-1}^{1} d\mu_2 \frac{b_1 F_2 + b_2/2 + b_{s^2} S_2/2 + \mu_2^2 f G_2}{b_1 + \mu_2^2 f} L_2(\mu_2) = -\left(F_2 - G_2 + \frac{b_2}{2b_1} + \frac{b_{s^2}}{2b_1} S_2 \right) \beta^{-3/2} [-3\sqrt{\beta} + (\beta + 3) \arctan \sqrt{\beta}]. \tag{42}$$

Similar expressions can be found for the second and third terms in the square bracket of (37). Putting everything together, we then obtain for the quadrupole,

$$Q_2^{\text{int}}(r,z) = \frac{r^{9/2}}{8\pi\sqrt{2}} \int_0^{2\pi/r} dk_1 k_1^2 \int_0^{2\pi/r} dk_2 k_2^2 \int_{-1}^{\nu_{\text{cut}}} d\nu \sqrt{\frac{P_L(|\mathbf{k}_1 + \mathbf{k}_2|, z) P_L(k_1, z)}{P_L(k_2, z)}} \sum_{i=1}^{3} j_2(\kappa_i r) \left(1 - \frac{3}{2} \frac{\rho_i^2}{\kappa_i^2} \right)$$
$$\times \left(F_2 - G_2 + \frac{b_2}{2b_1} + \frac{b_{s^2}}{2b_1} S_2 \right) (-\mathbf{k}_1 - \mathbf{k}_2, \mathbf{k}_1) \frac{5}{2\beta^{3/2}} (-3\sqrt{\beta} + (\beta + 3) \arctan \sqrt{\beta}), \tag{43}$$

where

$$\rho_1^2 = \rho_2^2 = k_1^2 (1 - \nu^2) \quad \text{and} \quad \rho_3^2 = 4\rho_1^2. \tag{44}$$

Equation (43) contains again three integrals that can be computed numerically.

3. The hexadecapole of the intrinsic contribution

The hexadecapole can be calculated in a very similar way as the quadrupole. The only difference is that the integral over ϕ_2 and φ in Eq. (41) contains Legendre polynomial of degree four instead of two. The resulting integral over μ_2 can again been done analytically, and we find

$$Q_4^{\text{int}}(r,z) = \frac{r^{9/2}}{8\pi\sqrt{2}} \int_0^{2\pi/r} dk_1 k_1^2 \int_0^{2\pi/r} dk_2 k_2^2 \int_{-1}^{\nu_{\text{cut}}} d\nu \sqrt{\frac{P_L(|\mathbf{k}_1+\mathbf{k}_2|,z)P_L(k_1,z)}{P_L(k_2,z)}} \left(F_2 - G_2 + \frac{b_2}{2b_1} + \frac{b_{s^2}}{2b_1} S_2 \right)(-\mathbf{k}_1-\mathbf{k}_2,\mathbf{k}_1)$$

$$\times \frac{9}{8\beta^{5/2}} \left[(3\beta^2+30\beta+35)\arctan\sqrt{\beta} - \left(\frac{55}{3}\beta+35\right)\sqrt{\beta} \right] \sum_{i=1}^3 j_4(\kappa_i r)\left(1 - 5\frac{\rho_i^2}{\kappa_i^2} + \frac{35}{8}\frac{\rho_i^4}{\kappa_i^4}\right). \tag{45}$$

4. General expression for the multipole Q_n of the intrinsic contribution

Following the same steps as for the monopole, quadrupole, and hexadecapole, one can derive a general expression for the multipole of order n. The detail of the derivation is presented in Appendix B. Here, we only give the final expression,

$$Q_{2n}^{\text{int}}(r,z) = \frac{r^{9/2}}{8\pi\sqrt{2}} \int_0^{2\pi/r} dk_1 k_1^2 \int_0^{2\pi/r} dk_2 k_2^2 \int_{-1}^{\nu_{\text{cut}}} d\nu \sqrt{\frac{P_L(|\mathbf{k}_1+\mathbf{k}_2|,z)P_L(k_1,z)}{P_L(k_2,z)}}$$

$$\times \frac{4n+1}{2} i^{2n} \mathcal{L}_{2n}(I) \sum_{i=1}^3 j_{2n}(\kappa_i r)\psi_{2n}\left(\frac{\rho_i}{\kappa_i}\right). \tag{46}$$

Here,

$$\mathcal{L}_{2n}(I) = 2^{2n} \sum_{m=0}^n \binom{2n}{2m}\binom{n+m-\frac{1}{2}}{2n} I_{2m}, \tag{47}$$

with

$$I_{2m} = \frac{2}{2m+1}\left\{ G_2(-\mathbf{k}_1-\mathbf{k}_2,\mathbf{k}_1) + \left(F_2 - G_2 + \frac{b_2}{2b_1} + \frac{b_{s^2}}{2b_1}S_2 \right)(-\mathbf{k}_1-\mathbf{k}_2,\mathbf{k}_1) {}_2F_1\left(1,\frac{1}{2}+m,\frac{3}{2}+m;-\beta\right) \right\}, \tag{48}$$

where ${}_2\mathcal{F}_1$ denotes the Gauss hypergeometric function and

$$\psi_{2n}\left(\frac{\rho_i}{\kappa_i}\right) = {}_2\mathcal{F}_1\left(-n, n+\frac{1}{2}, 1; \left(\frac{\rho_i}{\kappa_i}\right)^2\right), \tag{49}$$

with the ρ_i defined in Eq. (44).

B. Multipoles due to the mapping contribution

We now calculate the multipoles generated by the mapping kernel W_2^{map} in Eq. (27). We perform the same change of variables as in Sec. III A: $\{\theta_1, \phi_1, \theta_2, \phi_2\} \rightarrow \{\gamma, \varphi, \theta_2, \phi_2\}$, and we integrate analytically over φ, θ_2 and ϕ_2. All the contributions in Eq. (27) can be written as a sum of the following integrals:

$$\mathcal{I}_{nmm'} = \frac{1}{2(2\pi)^2} \int_0^\pi d\theta_2 \sin\theta_2 \int_0^{2\pi} d\phi_2 \int_0^{2\pi} d\varphi \frac{\mu_1^m \mu_2^{m'}}{1+\beta\mu_2^2} L_n(\hat{\boldsymbol{\kappa}}_i \cdot \mathbf{n}). \tag{50}$$

These integrals can be performed analytically. Their expression is given in Appendix C. The multipoles contain then three remaining integrals over k_1, k_2, and ν that can be performed numerically. As an example, here we write the expression for the monopole, but similar expressions can be derived for any multipole,

$$Q_0^{\text{map}}(r,z) = \frac{r^{9/2}}{8\pi\sqrt{2}} \int_0^{2\pi/r} dk_1 k_1^2 \int_0^{2\pi/r} dk_2 k_2^2 \int_{-1}^{\nu_{\text{cut}}} d\nu \sqrt{\frac{P_L(|\mathbf{k}_1+\mathbf{k}_2|,z)P_L(k_1,z)}{P_L(k_2,z)}} \sum_{i=1}^3 j_0(\kappa_i r)$$

$$\times \left\{ \frac{f}{2}\left(\frac{k_2}{k_1} - \frac{k_1 k_2}{k_{12}^2}\right)\mathcal{I}_{011} - \frac{f}{2}\frac{k_2^2}{k_{12}^2}\mathcal{I}_{002} + \frac{\beta f}{2}\frac{k_2^2}{k_{12}^2}\mathcal{I}_{022} + \frac{\beta f}{2}\frac{k_2^3}{k_1 k_{12}^2}\mathcal{I}_{013} \right\}, \tag{51}$$

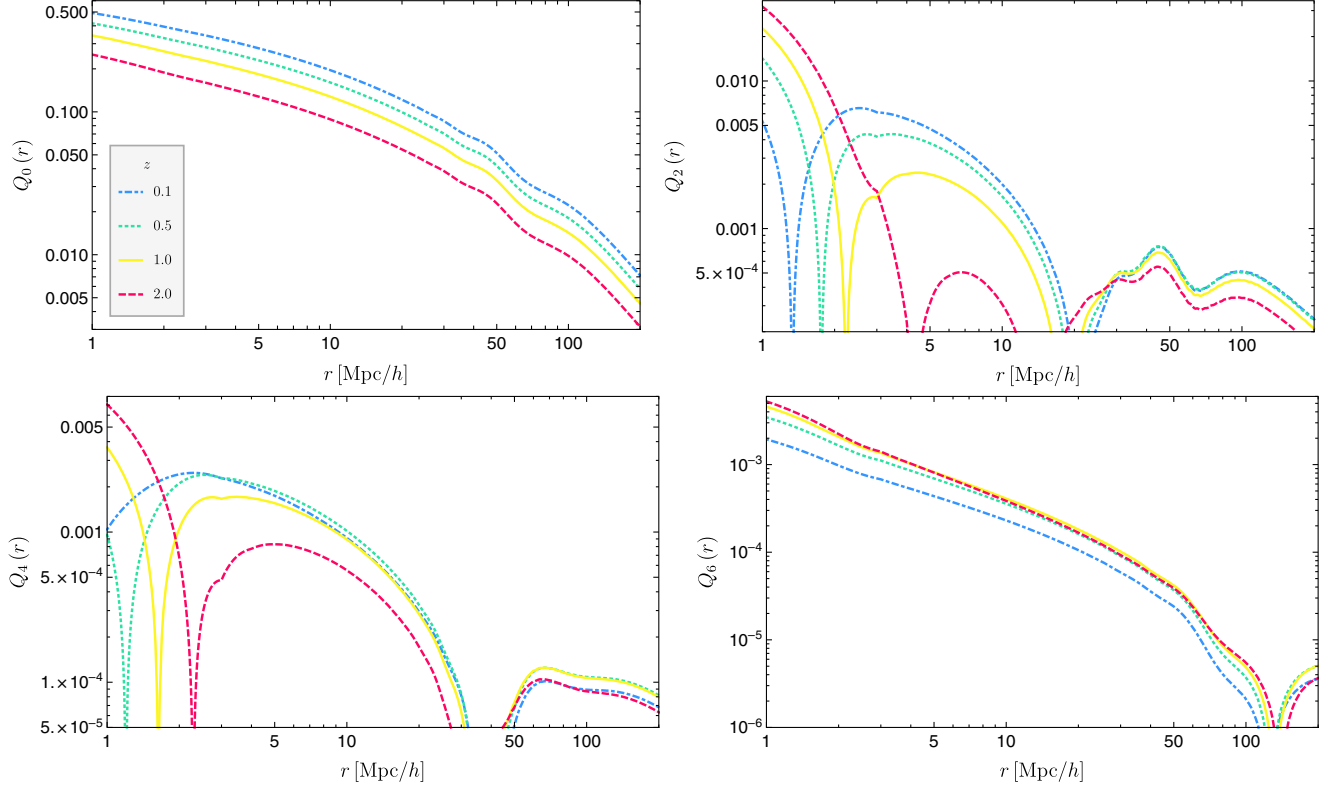where $k_{12} \equiv |\mathbf{k}_1 + \mathbf{k}_2|$.

FIG. 3. Multipoles of the line correlation function, plotted as a function of separation r, for redshift $z = 0.1$ to $z = 2$. The monopole is positive at all separations. The quadrupole, hexadecapole, and tetrahexadecapole change sign.

IV. RESULTS

We now calculate explicitly the multipoles of the line correlation function in a ΛCDM universe with parameters [54]: $\Omega_m = 0.3089$, $\Omega_b h^2 = 0.0223$, $h = 0.6774$, $n_s = 0.9667$, $\sigma_8 = 0.8159$. We choose as the fiducial value for the bias $b_1 = 1$, $b_2 = 0$, and $b_{s^2} = 0$, except for Fig. 5, where we show explicitly the impact of nonlinear bias on the multipoles. In Fig. 3, we show the monopole, quadrupole, hexadecapole, and tetrahexadecapole ($n = 6$) at different redshifts. These multipoles are the sum of the intrinsic contribution and the mapping contribution. The monopole decreases with redshift, whereas the quadrupole, hexadecapole, and tetrahexadecapole have a more complicated behavior. The redshift dependence is governed by the coupling kernels F_2 and G_2, by the linear power spectrum, and by the growth rate f, which enters in a different way in the different multipoles.

We see that the monopole dominates over the other multipoles by at least one order of magnitude. Note that the monopole is always positive, whereas the quadrupole, hexadecapole, and tetrahexadecapole change sign. The r dependence of the multipole n is governed by the sum of the spherical Bessel functions $j_n(\kappa_i r)$, weighted by different k- and ν-dependent prefactors. It is therefore not surprising that the multipoles can change sign. This behavior is not specific to the line correlation function: the monopole of the two-point correlation function in redshift space does indeed also change sign at large separation; see, e.g., [55]. Note that, as mentioned before, our results are obtained using second-order perturbation theory. At small scales, Fingers of God are expected to generate non-negligible corrections to the line correlation function and to change, consequently, its behavior.

In Fig. 4, we show the relative contribution due to redshift-space distortions

$$\Delta Q_n = \frac{Q_n - Q_n^{\text{no rsd}}}{Q_0^{\text{no rsd}}}, \qquad (52)$$

for $n = 0$, 2, 4, 6, and 8. Note that $Q_n^{\text{no rsd}}$ is equivalent to Eq. (30) for $\ell(r, z)$ in [18]. We see that redshift-space distortions generate a correction of up to 20% in the monopole, at small separation and high redshift. The quadrupole is roughly 5% of the monopole and the hexadecapole 1%. The tetrahexadecapole is always less than 0.5% of the monopole, apart at high redshift and very small separation where it reaches 2%. Most of the information about redshift-space distortions is therefore captured by the first three even multipoles.

In Fig. 5, we compare the different contributions to the multipoles at $z = 1$. We choose the value $b_1 = 2.1$ for the linear bias, as measured in [56], and we split the intrinsic
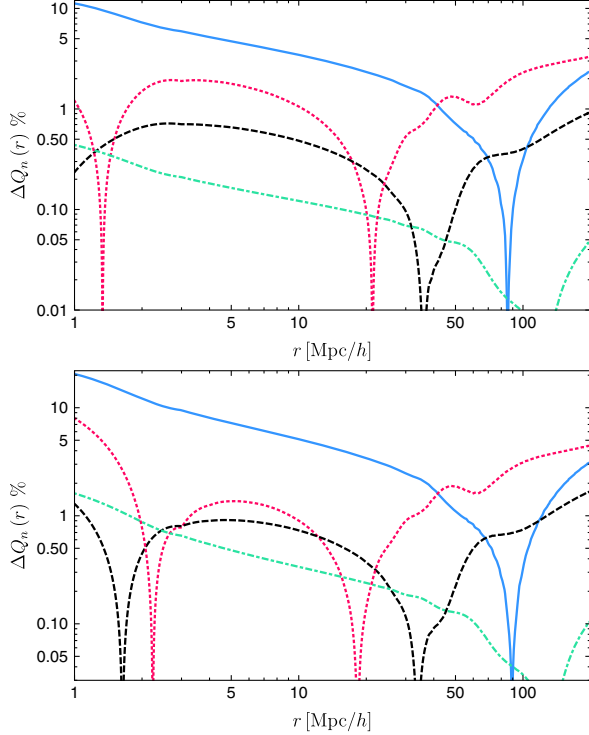
FIG. 4. Relative contribution due to redshift-space distortions (52) plotted as a function of separation r, at $z = 0.1$ (top panel) and $z = 1$ (bottom panel). The blue solid line shows the monopole contribution, the red dotted line the quadrupole contribution, the black dashed line the hexadecapole contribution, and the green dot-dashed line the tetrahexadecapole contribution.

contribution into: the redshift-space distortion part generated by the F_2 and G_2 kernels (blue line), the nonlinear bias contribution with $b_2 = 0.9$ (green line) [56], and the nonlocal bias contribution with $b_{s^2} = -4/7(b_1 - 1) = -0.63$ (yellow line) [43]. The mapping contribution is shown in red, and for the monopole, we also show separately the density contribution (purple line). As expected, the main contribution to the monopole is due to the density contribution F_2, which is intrinsically isotropic. The nonlocal bias contribution has a shape very similar to the density contribution, whereas the nonlinear bias contribution is more relevant at large separation. This is consistent with the results presented in Fig. 1 of [34] for the monopole. Comparing the intrinsic redshift-space distortion contribution (blue line) with the mapping contribution (red line), we see that the former dominates at large scales, whereas the latter is more important at small scales. This behavior is even more pronounced for the higher multipoles ($n = 2, 4,$ and 6), where we see that the mapping contribution is important mainly below 5 Mpc/h. For these higher multipoles, contrary to the monopole, the nonlocal bias contribution is strongly subdominant. This indicates that this contribution is mainly isotropic. The nonlinear bias contribution, on the other hand, contributes to all

multipoles, in a very similar way as the intrinsic redshift-space distortion contribution.

Comparing the amplitude of the density contribution in the monopole (purple line) with the intrinsic redshift-space distortions contribution in all multipoles (blue line), we see that the latter is significantly suppressed with respect to the former one. This can be understood by looking at the form of Eqs. (40), (43), and (45), where we see that the intrinsic redshift-space distortions contribution is always proportional to the *difference* between the density kernel F_2 and the velocity kernel G_2. This follows from the fact that the correlation between phases in Eq. (23) is proportional to the weighted bispectrum $b_\Delta \propto B_\Delta / \sqrt{P_\Delta P_\Delta P_\Delta}$. This weighted bispectrum probes the difference between the linear relation between V and δ and the nonlinear relation. If these relations are the same, then $F_2 = G_2$ and the function W_2^{int} defined in Eq. (26) reduces simply to F_2 (when $b_2 = b_{s^2} = 0$). We recover then the expression for the line correlation function in real space. Hence by measuring the line correlation function in redshift space, we probe the fact that the relation between the density δ and the peculiar velocity V is different at linear and at second order in perturbation theory. In other words, we probe the difference between the continuity and Euler equation at linear and second order in perturbation theory.

As such, the line correlation function is complementary to the two-point correlation function in redshift space. The two-point correlation function probes indeed the linear relation between density and velocity by measuring the growth rate f. The line correlation function adds information since it probes the nonlinear relation between the density and velocity by measuring the difference $F_2 - G_2$. This clearly shows that phase correlations encode a different type of information than the two-point correlation function. Modified theories of gravity generically modify both the growth rate f [57–59] and the coupling kernels F_2 and G_2 [49]. Hence, the line correlation function in redshift space is expected to be useful to constrain modifications of gravity.

In Fig. 6, we compare the contribution to the monopole (40) generated by the kernel F_2 only, by the kernel G_2, and by the difference $F_2 - G_2$. We see that the difference is significantly smaller than the individual contributions from F_2 and G_2. This explains the suppression of the redshift-space distortion signal, with respect to the signal in real space. Note that here we are using second-order perturbation theory, which does not account for the effect of Fingers of God at small scales. As shown in [11,12,38,39], those have a strong impact on the bispectrum in the nonlinear regime. In a future work, we will study the line correlation function beyond perturbation theory, accounting for the Fingers of God, to see if they enhance the multipoles.

In Fig. 7, we plot the prefactors for the intrinsic monopole, quadrupole, and hexadecapole, which depend on the growth rate $\beta = f/b$,
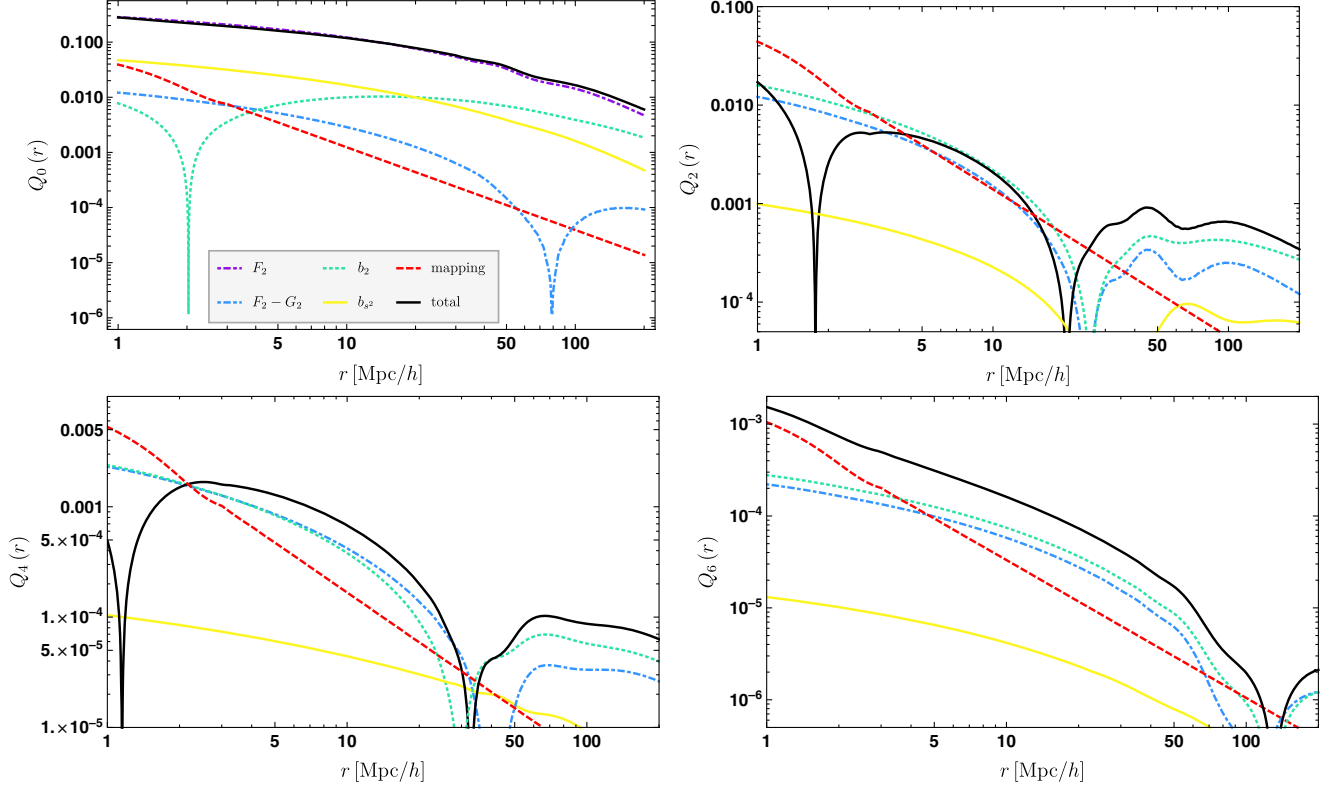
FIG. 5. Different contributions to the multipoles of the line correlation function at redshift $z = 1.0$. We plotted the density contribution F_2 (purple dot-dashed line), redshift-space distortion $F_2 - G_2$ (blue dot-dashed line) with linear bias $b_1 = 2.1$, the nonlinear bias contribution (green dotted line) with $b_2 = 0.9$, the nonlocal bias contribution (yellow solid line) with $b_{s^2} = -4/7(b_1 - 1) = -0.63$, the mapping contribution (red dashed line) and the total (black solid line).

$$A_0 = \frac{\arctan\sqrt{\beta}}{\sqrt{\beta}} - 1, \tag{53}$$

$$A_2 = \frac{5}{2\beta^{3/2}}[-3\sqrt{\beta} + (\beta + 3)\arctan\sqrt{\beta}], \tag{54}$$

$$A_4 = \frac{9}{8\beta^{5/2}}\left[-\left(\frac{55\beta}{3} + 35\right)\sqrt{\beta} + (3f^2 + 30f + 35)\arctan\sqrt{\beta}\right]. \tag{55}$$

We see that these prefactors evolve slowly with redshift, showing that the line correlation function is less sensitive than the two-point correlation function to variations in the growth rate. We also see that these prefactors are smaller
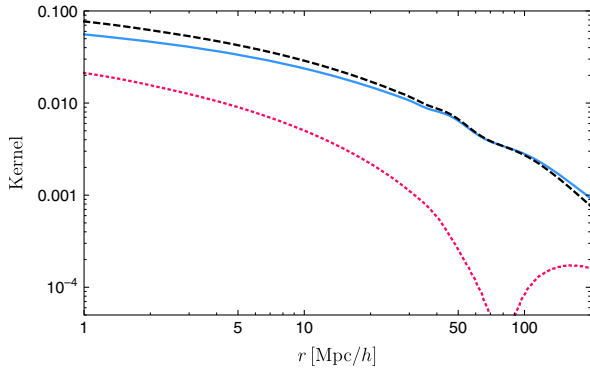

FIG. 6. Monopole of the line correlation function (40), at redshift $z = 1$, generated by the kernel F_2 (blue solid line), G_2 (black dashed line), and the difference $F_2 - G_2$ (red dotted line). The contributions from F_2 and G_2 are negative, while the difference is positive at small separations and negative at large separations.
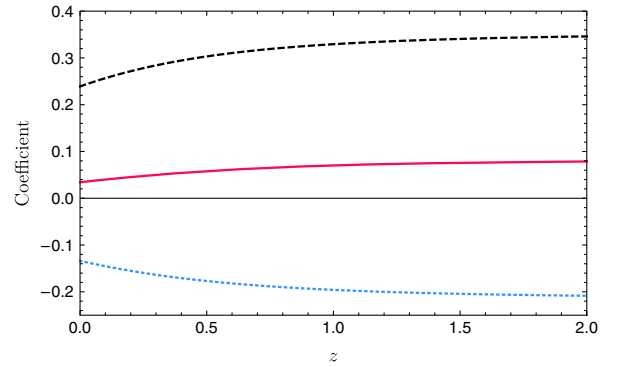

FIG. 7. Coefficients proportional to the growth rate $\beta = f/b$, in front of the monopole (53) (blue dotted line), quadrupole (54) (black dashed line), and hexadecapole (55) (red solid line) plotted as a function of redshift.
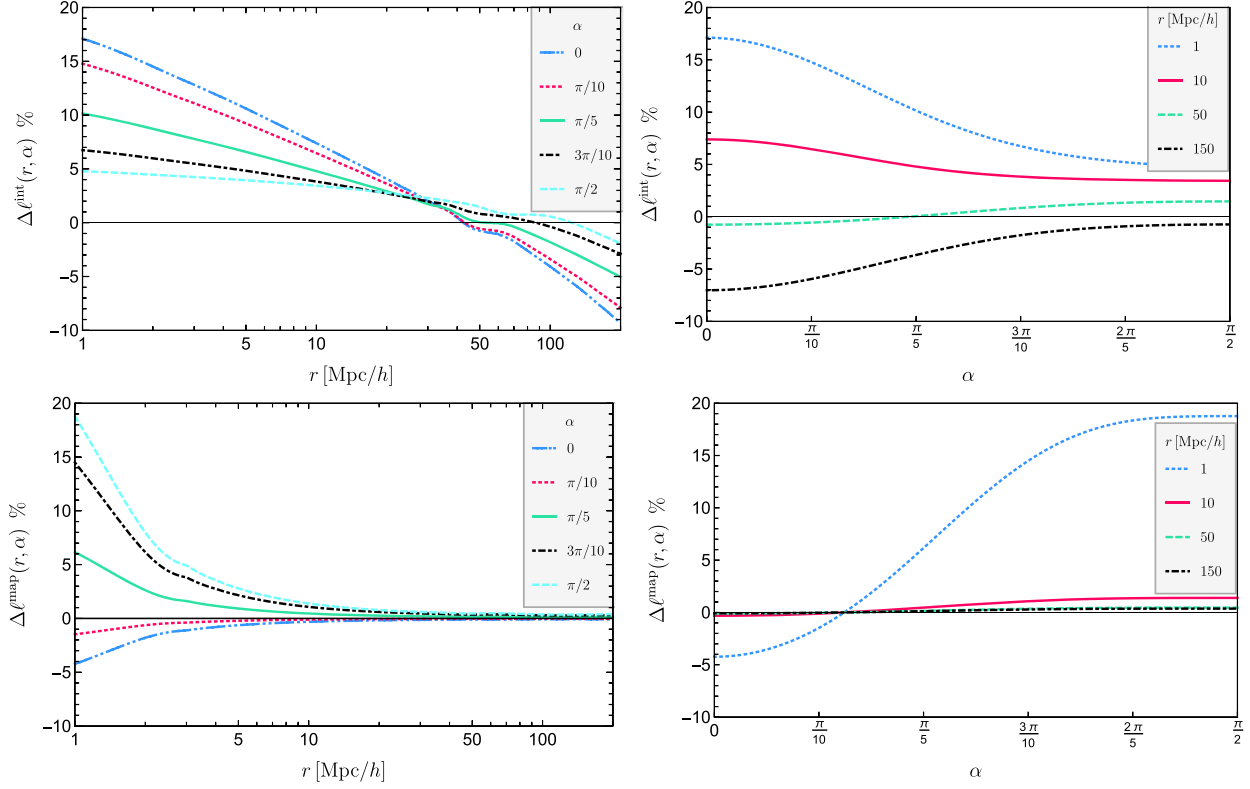
FIG. 8.   Relative contribution from redshift-space distortion (56) plotted as a function of separation r for fixed values of the orientation α (left panels) and as a function of the orientation α for fixed separation r (right panels). The plots are at redshift $z = 1$. The top panels show the intrinsic contribution, whereas the bottom panels show the mapping contribution.

than 1 at all redshift, which also explains why the redshift-space correction is significantly smaller than the density contribution.

Note that the different dependence of the multipoles in the growth rate is very interesting, since it provides a way of disentangling it from the parameter σ_8. The two-point correlation function measures indeed the combination $f\sigma_8$ (see, e.g., [8]). The monopole of the bispectrum has been shown to measure a different combination, $f^{0.43}\sigma_8$, which in combination with the two-point function allows us to disentangle f and σ_8 [56]. Here, we see from Eqs. (40), (43), and (45) that the multipoles of the line correlation function are sensitive to yet three other combinations of f and σ_8. Combining these measurements has therefore the potential to tighten the individual constraints on f and σ_8. In a future work, we will do a detail forecast on the constraints we expect from the line correlation function on f, σ_8, and the coupling kernels F_2 and G_2.

Finally, in Fig. 8, we show the relative contribution from redshift-space distortion as a function of the orientation[2] of the line α and the separation r,

$$\Delta\ell(r,\alpha,z) = \frac{\ell(r,\alpha,z) - \ell^{\text{no rsd}}(r,z)}{\ell^{\text{no rsd}}(r,z)}. \qquad (56)$$

We plot separately the intrinsic contribution (top panels, with $b_1 = 1$, $b_2 = 0$, and $b_{s^2} = 0$) and the mapping contribution (bottom panels). We see that the intrinsic contribution has the largest impact at small separation and when the three points are aligned with respect to the direction of observation ($\alpha = 0$). In this case, the contribution from redshift-space distortions can reach 17%. This reflects the fact that redshift-space distortions modify the apparent radial distance between galaxies but not their apparent angular separation. As a consequence, it is the largest when the galaxies are at different radial distances but in the same direction.

One would then naively expect that in the other extreme, i.e., when $\alpha = \pi/2$, the intrinsic contribution $\Delta\ell^{\text{int}}(r,\alpha,z)$ would vanish. This corresponds indeed to the case where the three points are at the same redshift, but in different directions. From the cyan dashed line in the top left panel of Fig. 8, we see however that $\Delta\ell^{\text{int}}(r,\pi/2,z) \neq 0$. This can be understood in the following way: suppose that the three pixels, which are at the same redshift, are all situated in an overdense region. As a consequence, the galaxies inside each pixel are falling toward the center of the pixel. The pixels in redshift space look therefore denser than they are

---

[2]Since the multipoles larger than $n = 6$ are negligible, we can write the line correlation function as $\ell(r,\alpha,z) = Q_0(r,z) + Q_2(r,z)L_2(\cos\alpha) + Q_4(r,z)L_4(\cos\alpha) + Q_6(r,z)L_6(\cos\alpha)$.

in real space. Now since the three pixels are situated in the same overdense region, this effect induces a correlation between the three pixels. This in turns generates an additional correlation between the phases of Δ_{int}. This effect is independent of the orientation of **r** with respect to **n**. It simply comes from the fact that correlated density fields generate correlated velocity fields. Hence, even though at $\alpha = \pi/2$ there is no change in the apparent distance between the pixels, there is still an effect due to the fact that the size of each pixel changes in a correlated way. Note that this effect is not specific to the line correlation function, but it also exists in the two-point correlation function of galaxies: the redshift-space two-point correlation function at $\alpha = \pi/2$ is not the same as the real-space two-point correlation function $\xi(r, \alpha = \pi/2) \neq \xi^{no\ rsd}(r)$.

Finally, from the bottom panels of Fig. 8, we see that the mapping contribution quickly decreases with separation, for all orientations. For a fix separation, the dependance in α is nontrivial, going from a negative contribution when the three points are aligned with **n**, to a positive contribution when the three points are perpendicular to **n**.

V. CONCLUSIONS

In this paper, we have derived an expression for the line correlation function in redshift space, which is valid at second order in perturbation theory. We have expanded the line correlation function in Legendre polynomials, and we have derived a generic expression for the multipoles Q_n. We have calculated explicitly the first multipoles in a ΛCDM universe, and we have found that the monopole, quadrupole, and hexadecapole encode almost all of the information in redshift space.

We have shown that the multipoles are sensitive to the difference $F_2 - G_2$, i.e., to the difference between the nonlinear evolution of the density field and the nonlinear evolution of the velocity field. As such, the line correlation function is highly complementary to the two-point correlation function, which is sensitive to the linear growth rate of the density and velocity fields. This shows that correlations between phases encode different information than the two-point correlation function. Our expressions for the multipoles further show that each of them is sensitive to a different combination of the growth rate f and of σ_8. Combining this with a measurement of the two-point correlation function, which is sensitive to the product $f\sigma_8$, can therefore break the degeneracy between these two parameters. In a future work, we will forecast how well this can be achieved with current and future surveys.

Our derivation relies on second-order perturbation theory. It is however well-known that redshift-space distortions are not fully described by the second-order coupling kernel G_2 even on mildly nonlinear scales [10–12,38,39]. In a future work, we will investigate how the multipoles change if we introduce nonlinear effects, like Fingers of God. We expect such effects to enhance the

redshift-space distortion signal, since they will increase the difference $F_2 - G_2$.

Finally, let us note that the line correlation function targets a very particular choice of phase correlations, namely those that appear along a line, i.e., along filaments. It may be interesting to investigate other configurations, where the redshift-space distortions signal may be enhanced with respect to the real-space signal.

APPENDIX A: DERIVATION OF Δ AT SECOND ORDER

The overdensity of galaxies is given by

$$\Delta(\mathbf{n}, z) = \frac{N(\mathbf{n}, z) - \bar{N}(z)}{\bar{N}(z)} = \frac{\rho_g(\mathbf{n}, z)\mathcal{V}(\mathbf{n}, z) - \bar{\rho}_g(z)\bar{\mathcal{V}}(z)}{\bar{\rho}_g(z)\bar{\mathcal{V}}(z)},$$

(A1)

where $N(\mathbf{n}, z)$ denotes the number of galaxies detected in a pixel of volume $\mathcal{V}(\mathbf{n}, z)$, situated at redshift z, and in direction **n**, and $\rho_g(\mathbf{n}, z)$ is the energy density of galaxies in that pixel. Quantities with a bar refer to the average over directions, at a given redshift. At second order in perturbation theory, we obtain

$$\Delta^{(2)}(\mathbf{n}, z) = \delta_g^{(2)}(\mathbf{n}, z) + \frac{\delta\mathcal{V}^{(2)}(\mathbf{n}, z)}{\bar{\mathcal{V}}(z)}$$

$$+ \delta_g^{(1)}(\mathbf{n}, z)\frac{\delta\mathcal{V}^{(1)}(\mathbf{n}, z)}{\bar{\mathcal{V}}(z)}.$$
(A2)

Here, $\delta_g^{(2)}$ and $\delta\mathcal{V}^{(2)}$ are expressed in term of the observed redshift z. To calculate these quantities, we start from their expression written as a function of conformal time η, and we use that a fix η is directly related to a fix background redshift $\bar{z} = \frac{a_0}{a} - 1$, where a_0 denotes the scale factor today. We have

$$\mathcal{V}(\mathbf{n}, \eta) = \mathcal{V}(\mathbf{n}, \bar{z}) \simeq \bar{\mathcal{V}}(\bar{z}) + \delta\mathcal{V}^{(1)}(\mathbf{n}, \bar{z}) + \delta\mathcal{V}^{(2)}(\mathbf{n}, \bar{z})$$

$$\simeq \bar{\mathcal{V}}(z) - \frac{\partial\bar{\mathcal{V}}}{\partial z}\delta z + \frac{1}{2}\frac{\partial^2\bar{\mathcal{V}}}{\partial z^2}(\delta z)^2 - \frac{\partial\delta\mathcal{V}^{(1)}}{\partial z}\delta z + \delta\mathcal{V}^{(2)},$$
(A3)

where to obtain the second line we have used that $\bar{z} = z - \delta z$ and we have Taylor expanded $\mathcal{V}$ around z up to second order. We are interested in the dominant contributions to

$\Delta^{(2)}$, i.e., those with the maximum number of radial derivatives. We can therefore neglect the second and third term in the second line of (A3). For the fourth term, we rewrite the derivative with respect to z as a derivative with respect to the comoving distance coordinate $\chi = \eta_O - \eta$, and we obtain at second order,

$$
\begin{aligned}
\delta\mathcal{V}^{(2)} &= \delta\mathcal{V}^{(2)}(\mathbf{n}, z) - \frac{1}{\mathcal{H}}\partial_\chi\delta\mathcal{V}^{(1)}\frac{\delta z}{1 + \bar{z}} \\
&= \delta\mathcal{V}^{(2)}(\mathbf{n}, z) - \frac{1}{\mathcal{H}}\partial_\chi\delta\mathcal{V}^{(1)}(\mathbf{v}^{(1)}\cdot\mathbf{n}),
\end{aligned} \quad \text{(A4)}
$$

where we have used that the dominant contribution to the redshift perturbation is due to the Doppler effect. The dominant contribution to the volume perturbation is due to redshift-space distortions. It reads

$$
\frac{\delta\mathcal{V}}{\bar{\mathcal{V}}} = -\frac{1}{\mathcal{H}}\partial_\chi\left(\frac{\delta z}{1 + \bar{z}}\right). \quad \text{(A5)}
$$

Doing a similar expansion for $\delta\rho_g^{(2)}$ and inserting this into Eq. (A2), we obtain

$$
\begin{aligned}
\Delta^{(2)}(\mathbf{n}, z) = {} & \delta_g^{(2)} - \frac{1}{\mathcal{H}}\partial_\chi(\mathbf{v}^{(2)}\cdot\mathbf{n}) \\
& - \frac{1}{\mathcal{H}}\delta_g^{(1)}\partial_\chi(\mathbf{v}^{(1)}\cdot\mathbf{n}) - \frac{1}{\mathcal{H}}\partial_\chi\delta_g^{(1)}(\mathbf{v}^{(1)}\cdot\mathbf{n}) \\
& + \frac{1}{\mathcal{H}^2}\partial_\chi[\partial_\chi(\mathbf{v}^{(1)}\cdot\mathbf{n})(\mathbf{v}^{(1)}\cdot\mathbf{n})].
\end{aligned} \quad \text{(A6)}
$$

We call the first line the intrinsic contribution, since it is due to the intrinsic nonlinear evolution of the galaxy density and peculiar velocity, and the second and third line the mapping contribution, since it is generated by the nonlinear mapping between real space and redshift space. Since Δ is expressed in terms of the observed redshift z and the direction of the incoming photon $\mathbf{n}$, we can directly Fourier transform this expression with respect to the observed coordinate $\mathbf{x}_{\text{obs}} = \chi(z)\mathbf{n}$ to obtain Eq. (16).

An alternative way of deriving $\Delta(\mathbf{k})$ which is often presented in the literature [10] is to do a change of variable directly in the Fourier transform. We have

$$
\Delta(\mathbf{k}) = \frac{1}{(2\pi)^3}\int d^3\mathbf{x}_{\text{obs}}\Delta(\mathbf{x}_{\text{obs}})e^{-i\mathbf{k}\cdot\mathbf{x}_{\text{obs}}}. \quad \text{(A7)}
$$

Since the number of galaxies in a given pixel is conserved by redshift-space distortions, we can write $(1+\Delta(\mathbf{x}_{\text{obs}}))d^3\mathbf{x}_{\text{obs}} = (1+\delta_g(\mathbf{x}))d^3\mathbf{x}$. Using that $d^3\mathbf{x}_{\text{obs}}/d^3\mathbf{x} = \partial_\chi(\mathbf{v}\cdot\mathbf{n})/\mathcal{H}$, we obtain

$$
\Delta(\mathbf{x}_{\text{obs}})d^3\mathbf{x}_{\text{obs}} = \left(\delta_g(\mathbf{x}) - \frac{1}{\mathcal{H}}\partial_\chi(\mathbf{v}\cdot\mathbf{n})\right)d^3\mathbf{x}. \quad \text{(A8)}
$$

Inserting this into (A7) and using that $\mathbf{x}_{\text{obs}} = \mathbf{x} + (\mathbf{v}\cdot\mathbf{n})\mathbf{n}/\mathcal{H}$, we obtain

$$
e^{-i\mathbf{k}\cdot\mathbf{x}_{\text{obs}}} = e^{-i\mathbf{k}\cdot\mathbf{x} - i(\mathbf{v}\cdot\mathbf{n})(\mathbf{k}\cdot\mathbf{n})/\mathcal{H}} \quad \text{(A9)}
$$

$$
\simeq e^{-i\mathbf{k}\cdot\mathbf{x}}\left(1 - \frac{i}{\mathcal{H}}(\mathbf{v}\cdot\mathbf{n})(\mathbf{k}\cdot\mathbf{n})\right) \quad \text{(A10)}
$$

and

$$
\begin{aligned}
\Delta^{(2)}(\mathbf{k}) = {} & \delta_g^{(2)}(\mathbf{k}) - \frac{1}{\mathcal{H}}(\hat{\mathbf{k}}\cdot\mathbf{n})^2 V^{(2)}(\mathbf{k}) \\
& - i(\mathbf{k}\cdot\mathbf{n})\int\frac{d^3\mathbf{x}}{(2\pi)^3}e^{-i\mathbf{k}\cdot\mathbf{x}}\left(\delta_g^{(1)} - \frac{\partial_\chi}{\mathcal{H}}(\mathbf{v}^{(1)}\cdot\mathbf{n})\right) \\
& \times (\mathbf{v}^{(1)}\cdot\mathbf{n}).
\end{aligned} \quad \text{(A11)}
$$

The first line is the intrinsic contribution. For the second line, we Fourier transform $\delta^{(1)}$ and $\mathbf{v}^{(1)}$ and we integrate over $\mathbf{x}$. We obtain then the mapping contribution in Fourier space, Eq. (16). We see that the two approaches give the same result in Fourier space.

APPENDIX B: CALCULATION OF THE INTRINSIC MULTIPOLES Q_n^{int}

In Sec. III, we have performed a multipole expansion for the line correlation function. All the information of our statistical measure $\ell(\mathbf{r}, z)$ can be encoded in a (infinite) sum of multipoles $Q_n(r, z)$ given by (37). Here we show how three of the six integrals in this expression can be solved analytically for any order of multipole Q_n, namely the angular integrals θ_2, ϕ_2, and φ. The multipole Q_n contains an intrinsic and a mapping contribution; here we present the calculation for the intrinsic contribution Q_n^{int}.

Since only the kernel W_2^{int} and the Legendre polynomial L_n are functions of these angles, the challenge is to solve the following expression:

$$
\begin{aligned}
M_n^{\kappa_i} = {} & \int_0^\pi \sin\theta_2 d\theta_2 W_2^{\text{int}}(-\mathbf{k}_1 - \mathbf{k}_2, \mathbf{k}_1, \mathbf{k}_2, \mathbf{n}) \\
& \times \int_0^{2\pi} d\phi_2 \int_0^{2\pi} d\varphi L_n(\hat{\boldsymbol{\kappa}}_i\cdot\mathbf{n}).
\end{aligned} \quad \text{(B1)}
$$

The kernel W_2^{int} is provided by (27) and the vectors $\boldsymbol{\kappa}_i$ are defined in (34)–(36). The angles $\hat{\boldsymbol{\kappa}}_i\cdot\mathbf{n}$ can be written as

$$
\hat{\boldsymbol{\kappa}}_i\cdot\mathbf{n} \equiv \cos\theta_{\kappa_i} = \frac{\rho_i\sin\theta_2\cos(\varphi - \phi_2) + \varrho_i\cos\theta_2}{\kappa_i}, \quad \text{(B2)}
$$

where

$$
\begin{aligned}
\rho_1 &= -k_1\sin\gamma, & \varrho_1 &= k_1\cos\gamma - k_2, \\
\rho_2 &= -k_1\sin\gamma, & \varrho_2 &= k_1\cos\gamma + 2k_2, \\
\rho_3 &= 2k_1\sin\gamma, & \varrho_3 &= -2k_1\cos\gamma - k_2,
\end{aligned} \quad \text{(B3)}
$$

with constraint $\kappa_i^2 = \rho_i^2 + \varrho_i^2$.

In order to solve the integrals, we express the Legendre polynomials as

$$L_n(\hat{\boldsymbol{\kappa}}_i \cdot \mathbf{n}) = 2^n \sum_{m=0}^{n} \binom{n}{m} \binom{\frac{n+m-1}{2}}{n} \cos^m \theta_{\kappa_i}. \qquad \text{(B4)}$$

Because of the binomial coefficients, the only terms that contribute to the sum will be those with the same parity as n. Using the binomial expansion, $\cos^a \theta_{\kappa_i}$ can be rewritten as

$$\cos^m \theta_{\kappa_i} = \kappa_i^{-m} \sum_{u=0}^{m} \binom{m}{u} (\varrho_i \cos \theta_2)^{m-u} (\rho_i \sin \theta_2)^u$$
$$\times \cos^u(\varphi - \phi_2). \qquad \text{(B5)}$$

Therefore, the integrals over the axial angles ϕ_2 and φ can be trivially solved, and it yields

$$\int_0^{2\pi} d\phi_2 \int_0^{2\pi} d\varphi \cos^u(\varphi - \phi_2)$$
$$= \frac{1 + (-1)^u}{2} (2\pi)^2 \binom{(u-1)/2}{-1/2}. \qquad \text{(B6)}$$

The integral over θ_2 takes the form[3]

$$\int_0^{\pi} d\theta_2 \sin \theta_2 \frac{bF_2 + b_2/2 + b_{s^2}S_2/2 + \cos^2(\theta_2)fG_2}{b + \cos^2(\theta_2)f}$$
$$\times \cos^{m-u}(\theta_2) \sin^u(\theta_2). \qquad \text{(B7)}$$

These two expressions above reveal an important feature about the parity of LCF. First, Eq. (C7) tells us that only even values of u contribute to the sum (C5). Second, due to the orthogonality of the trigonometric functions, Eq. (B7) will not vanish if and only if $m - u$ is even, which implies that m must also be even. Thus, we conclude that in the multipole expansion (37), only even multipoles contribute to the sum. This reflects the fact that the line correlation function is symmetric under the exchange of the three galaxies on the line.

Thereby, without loss of generality, one can consider a relabeling: $n \to 2n$, $m \to 2m$, and $u \to 2u$. We can then use that $\varrho_i^{2(m-u)} = (\kappa_i^2 - \rho_i^2)^{m-u}$, so that

$$\kappa_i^{-2m} \varrho_i^{2(m-u)} \rho_i^{2u} = \sum_{w=0}^{m-u} \binom{m-u}{w} (-1)^w \left(\frac{\rho_i}{\kappa_i}\right)^{2(u+w)}. \qquad \text{(B8)}$$

In the interval $\theta_2 \in [0, \pi]$, the sine function can be written as $\sin \theta_2 = \sqrt{1 - \cos^2(\theta_2)}$, and consequently,

---

[3]To simplify the notation, we drop the argument in F_2, S_s and G_2 which are both functions of $(-\mathbf{k}_1 - \mathbf{k}_2, \mathbf{k}_1)$.

$$\sin^{2u}(\theta_2) = \sum_{v=0}^{u} \binom{u}{v} (-1)^v \cos^{2v}(\theta_2). \qquad \text{(B9)}$$

We are now able to solve the integral over θ_2, which is of the form,

$$\int_{-1}^{1} d\mu_2 \frac{bF_2 + b_2/2 + b_{s^2}S_2/2 + \mu_2^2 fG_2}{b + \mu_2^2 f} \mu_2^{2j}$$
$$= \frac{2}{j+1} \left[G_2 + \left(F_2 - G_2 + \frac{b_2}{2b_1} + \frac{b_{s^2}}{2b_1} S_2 \right) \right.$$
$$\left. \times {}_2\mathcal{F}_1 \left(1, \frac{1}{2} + j, \frac{3}{2} + j; -\beta \right) \right], \qquad \text{(B10)}$$

where in our case $j = m + v - u$. Here, ${}_2\mathcal{F}_1$ denotes the Gauss hypergeometric function defined by

$${}_2\mathcal{F}_1(a, b, c; z) = \sum_{n=0}^{\infty} \frac{(a)_n (b)_n}{(c)_n} \frac{z^n}{n!}, \qquad \text{(B11)}$$

where $(a)_n = \Gamma(a+n)/\Gamma(a)$ is the Pochhammer symbol. Finally, collecting all these results, $M_{2n}^{\kappa_i}$ can be written as

$$M_{2n}^{\kappa_i} = 2(2\pi)^2 2^{2n} \sum_{m=0}^{n} \sum_{u=0}^{m} \sum_{w=0}^{m-u} \sum_{v=0}^{u} \binom{2n}{2m} \binom{n+m-\frac{1}{2}}{2n}$$
$$\times \binom{2m}{2u} \binom{u-\frac{1}{2}}{-\frac{1}{2}} \binom{m-u}{w} \binom{u}{v} (-1)^{w+v} \left(\frac{\rho_i}{\kappa_i}\right)^{2(u+w)}$$
$$\times \frac{1}{2(m+v-u)+1} \left\{ G_2(-\mathbf{k}_1 - \mathbf{k}_2, \mathbf{k}_1) \right.$$
$$+ \left[F_2 - G_2 + \frac{b_2}{2b_1} + \frac{b_{s^2}}{2b_1} S_2 \right] (-\mathbf{k}_1 - \mathbf{k}_2, \mathbf{k}_1)$$
$$\left. \times {}_2\mathcal{F}_1 \left(1, \frac{1}{2} + m + v - u, \frac{3}{2} + m + v - u; -\beta \right) \right\}. \qquad \text{(B12)}$$

This expression can be further simplified through a long algebraic manipulation and indices relabeling, and we obtain

$$M_{2n}^{\kappa_i} = (2\pi)^2 \mathcal{L}_{2n}(I) \psi_{2n} \left(\frac{\rho_i}{\kappa_i}\right), \qquad \text{(B13)}$$

where

$$\mathcal{L}_{2n}(I) = 2^{2n} \sum_{m=0}^{n} \binom{2n}{2m} \binom{n+m-\frac{1}{2}}{2n} I_{2m} \qquad \text{(B14)}$$

with

$$I_{2m} = \frac{2}{2m+1} \left\{ G_2(-\mathbf{k}_1 - \mathbf{k}_2, \mathbf{k}_1) \right.$$

$$+ \left[F_2 - G_2 + \frac{b_2}{2b_1} + \frac{b_{s^2}}{2b_1} S_2 \right] (-\mathbf{k}_1 - \mathbf{k}_2, \mathbf{k}_1)$$

$$\left. \times {}_2\mathcal{F}_1 \left(1, \frac{1}{2} + m, \frac{3}{2} + m; -\beta \right) \right\}, \tag{B15}$$

and

$$\psi_{2n}\left(\frac{\rho_i}{\kappa_i}\right) = {}_2\mathcal{F}_1\left(-n, n + \frac{1}{2}, 1; \left(\frac{\rho_i}{\kappa_i}\right)^2\right). \tag{B16}$$

This shows that the multipoles can be calculated from an expression (46).

APPENDIX C: CALCULATION OF THE MAPPING MULTIPOLES Q_n^{map}

The calculation for the mapping contribution Q_n^{map} is similar to what was done for the intrinsic contribution. Here, the expression is

$$\mathcal{M}_n^{\kappa_i} = \int_0^\pi \sin\theta_2 d\theta_2 W_2^{\mathrm{map}}(-\mathbf{k}_1 - \mathbf{k}_2, \mathbf{k}_1, \mathbf{k}_2, \mathbf{n})$$

$$\times \int_0^{2\pi} d\phi_2 \int_0^{2\pi} d\varphi L_n(\hat{\boldsymbol{\kappa}}_i \cdot \mathbf{n}), \tag{C1}$$

with the kernel W_2^{map} given by (26). For this case, it is better to express $\mathcal{M}_n^{\kappa_i}$ as a linear combination of integrals of the type

$$\mathcal{I}_{nmm'} = \frac{1}{2(2\pi)^2} \int_0^\pi \sin\theta_2 d\theta_2 \int_0^{2\pi} d\phi_2 \int_0^{2\pi} d\varphi$$

$$\times \frac{\mu_1^m \mu_2^{m'}}{1 + \beta\mu_2^2} L_n(\hat{\boldsymbol{\kappa}}_i \cdot \mathbf{n}), \tag{C2}$$

since the kernel is a sum of powers of μ_1 and μ_2 with the denominator $1 + \beta\mu_2^2$. From (26), it is easy to see the relation between $\mathcal{M}_n^{\kappa_i}$ and $\mathcal{I}_{nmm'}$,

$$\mathcal{M}_n^{\kappa_i} = \frac{f}{2}\left(\frac{k_2}{k_1} - \frac{k_1 k_2}{k_{12}^2}\right)\mathcal{I}_{n11} - \frac{f}{2}\frac{k_2^2}{k_{12}^2}\mathcal{I}_{n02}$$

$$+ \frac{\beta f}{2}\frac{k_2^2}{k_{12}^2}\mathcal{I}_{n22} + \frac{\beta f}{2}\frac{k_2^3}{k_1 k_{12}^2}\mathcal{I}_{n13}, \tag{C3}$$

with $k_{12} \equiv |\mathbf{k}_1 + \mathbf{k}_2|$. To calculate the terms $\mathcal{I}_{nmm'}$, one can use the same tricks already used previously, namely express the Legendre polynomials as

$$L_n(\hat{\boldsymbol{\kappa}}_i \cdot \mathbf{n}) = 2^n \sum_{b=0}^n \binom{n}{b} \binom{\frac{n+b-1}{2}}{n} \cos^b\theta_{\kappa_i}, \tag{C4}$$

such that

$$\cos^b\theta_{\kappa_i} = \kappa_i^{-b} \sum_{c=0}^b \binom{b}{c} (\varrho_i \cos\theta_2)^{b-c} (\rho_i \sin\theta_2)^c$$

$$\times \cos^c(\varphi - \phi_2). \tag{C5}$$

Meanwhile due the change of variables performed in Sec. III A, one obtains the relation $\mu_1 \equiv \cos\theta_1 = \cos\gamma\cos\theta_2 - \sin\gamma\sin\theta_2\cos(\varphi - \phi_2)$. Consequently,

$$\mu_1^m = \sum_{a=0}^m \binom{m}{a} (-1)^a \cos^{m-a}\gamma \sin^a\gamma$$

$$\times \cos^{m-a}\theta_2 \sin^a\theta_2 \cos^a(\varphi - \phi_2). \tag{C6}$$

In this way, the integration over the angles ϕ_2 and φ gives

$$\int_0^{2\pi} d\phi_2 \int_0^{2\pi} d\varphi \cos^{a+c}(\varphi - \phi_2)$$

$$= \frac{1 + (-1)^{a+c}}{2} (2\pi)^2 \binom{\frac{a+c-1}{2}}{-1/2}, \tag{C7}$$

implying that $a + c$ must be even; otherwise, those integrals vanish. That result allows us to rewrite the sin function as

$$\sin^{a+c}\theta_2 = (1 - \mu_2^2)^{\frac{a+c}{2}} = \sum_{d=0}^{\frac{a+c}{2}} \binom{\frac{a+c}{2}}{d} (-1)^d \mu_2^{2d}, \tag{C8}$$

since $\theta_2 \in [0, \pi]$, i.e., $\sin\theta_2 \in [0, 1]$. So the integration over θ_2 can be fully written in term of μ_2, and it has the form

$$\int_{-1}^1 d\mu_2 \frac{\mu_2^X}{1 + \beta\mu_2^2}$$

$$= \frac{1 + (-1)^X}{1 + X} {}_2\mathcal{F}_1\left(1, \frac{1+X}{2}, \frac{3+X}{2}; -\beta\right). \tag{C9}$$

Thereby, the terms $\mathcal{I}_{nmm'}$ can be generally written as

$$\mathcal{I}_{nmm'} = 2^{2n} \sum_{a=0}^m \sum_{b=0}^n \sum_{c=0}^b \sum_{d=0}^{\frac{a+c}{2}} \binom{m}{a}\binom{n}{b}\binom{\frac{n+b-1}{2}}{n}$$

$$\times \binom{b}{c}\binom{\frac{a+c}{2}}{d}\binom{\frac{a+c-1}{2}}{-1/2}(-1)^{a+d}\frac{1+(-1)^{a+c}}{2}$$

$$\times \cos^{m-a}\gamma\sin^a\gamma\left(\frac{\varrho_i}{\kappa_i}\right)^b\left(\frac{\rho_i}{\varrho_i}\right)^c$$

$$\times \frac{1 + (-1)^X}{2(1+X)} {}_2\mathcal{F}_1\left(1, \frac{1+X}{2}, \frac{3+X}{2}; -\beta\right), \tag{C10}$$

with $X \equiv m + m' - a + b - c + 2d$. For sake of simplicity, we present below only the terms that contribute to the monopole and the quadrupole,

$$\mathcal{I}_{000} = H_0,$$

$$\mathcal{I}_{002} = \frac{H_2}{3},$$

$$\mathcal{I}_{011} = \frac{H_2}{3}\cos\gamma,$$

$$\mathcal{I}_{022} = \frac{H_4}{5}\cos^2\gamma + \frac{5H_2 - 3H_4}{30}\sin^2\gamma$$

$$\mathcal{I}_{013} = \frac{H_4}{5}\cos\gamma,$$

$$\mathcal{I}_{200} = \left[1 - \frac{3}{2}\left(\frac{\rho_i}{\kappa_i}\right)^2\right]\frac{H_2 - H_0}{2},$$

$$\mathcal{I}_{202} = \left[1 - \frac{3}{2}\left(\frac{\rho_i}{\kappa_i}\right)^2\right]\frac{9H_4 - 5H_2}{30},$$

$$\mathcal{I}_{211} = \left[1 - \frac{3}{2}\left(\frac{\rho_i}{\kappa_i}\right)^2\right]\frac{9H_4 - 5H_2}{30}\cos\gamma + \frac{\rho_i\varrho_i}{\kappa_i^2}\frac{3H_4 - 5H_2}{10}\sin\gamma$$

$$\mathcal{I}_{222} = \left[1 - \frac{3}{2}\left(\frac{\rho_i}{\kappa_i}\right)^2\right]\frac{15H_6 - 7H_4}{70}\cos^2\gamma + \left\{\left[1 - \frac{3}{2}\left(\frac{\rho_i}{\kappa_i}\right)^2\right]\frac{-H_6 + 2H_4 - H_2}{8} + \frac{15H_6 - 42H_4 + 35H_2}{840}\right\}\sin^2\gamma$$

$$+ \frac{\rho_i\varrho_i}{\kappa_i^2}\frac{15H_6 - 21H_4}{35}\cos\gamma\sin\gamma,$$

$$\mathcal{I}_{213} = \left[1 - \frac{3}{2}\left(\frac{\rho_i}{\kappa_i}\right)^2\right]\frac{15H_6 - 7H_4}{70} + \frac{\rho_i\varrho i}{\kappa_i^2}\frac{15H_6 - 21H_4}{70}\sin\gamma,$$

where $H_X \equiv {}_2\mathcal{F}_1(1, (1 + X)/2, (3 + X)/2; -\beta)$. For higher multipoles, the expressions are more complicated but they can be straightforwardly obtained by Eq. (C10).

[1] D. H. Jones *et al.*, Mon. Not. R. Astron. Soc. **399**, 683 (2009).

[2] K. N. Abazajian *et al.* (SDSS Collaboration), Astrophys. J. Suppl. Ser. **182**, 543 (2009).

[3] D. Parkinson, S. Riemer-Sørensen, C. Blake, G. B. Poole, T. M. Davis, S. Brough, M. Colless, C. Contreras, W. Couch, S. Croom *et al.*, Phys. Rev. D **86**, 103518 (2012).

[4] M. Scodeggio, L. Guzzo, B. Garilli, B. R. Granett, M. Bolzonella, S. de la Torre, U. Abbas, C. Adami, S. Arnouts, D. Bottini *et al.*, Astron. Astrophys. **609**, A84 (2018).

[5] S. Alam, F. D. Albareti, C. Allende Prieto, F. Anders, S. F. Anderson, T. Anderton, B. H. Andrews, E. Armengaud, É. Aubourg, S. Bailey *et al.*, Astrophys. J. **219**, 12 (2015).

[6] N. Kaiser, Mon. Not. R. Astron. Soc. **227**, 1 (1987).

[7] A. J. S. Hamilton, in *Ringberg Workshop on Large Scale Structure Ringberg, Germany, 1996* (1997), https://inspirehep.net/record/971195.

[8] S. Alam *et al.* (BOSS Collaboration), Mon. Not. R. Astron. Soc. **470**, 2617 (2017).

[9] A. G. Sanchez *et al.* (BOSS Collaboration), Mon. Not. R. Astron. Soc. **464**, 1640 (2017).

[10] R. Scoccimarro, H. M. P. Couchman, and J. A. Frieman, Astrophys. J. **517**, 531 (1999).

[11] E. Gaztanaga and R. Scoccimarro, Mon. Not. R. Astron. Soc. **361**, 824 (2005).

[12] H. Gil-Marín, C. Wagner, J. Norena, L. Verde, and W. Percival, J. Cosmol. Astropart. Phys. 12 (2014) 029.

[13] C. Hikage, Y. Suto, I. Kayo, A. Taruya, T. Matsubara, M. S. Vogeley, F. Hoyle, J. R. Gott, III, and J. Brinkmann (SDSS Collaboration), Publ. Astron. Soc. Jpn. **54**, 707 (2002).

[14] S. Codis, C. Pichon, D. Pogosyan, F. Bernardeau, and T. Matsubara, Mon. Not. R. Astron. Soc. **435**, 531 (2013).

[15] M. White, J. Cosmol. Astropart. Phys. 11 (2016) 057.

[16] M. Scrimgeour *et al.*, Mon. Not. R. Astron. Soc. **425**, 116 (2012).

[17] D. Obreschkow, C. Power, M. Bruderer, and C. Bonvin, Astrophys. J. **762**, 115 (2013).

[18] R. Wolstenhulme, C. Bonvin, and D. Obreschkow, Astrophys. J. **804**, 132 (2015).

[19] R. J. Scherrer, A. L. Melott, and S. F. Shandarin, Astrophys. J. **377**, 29 (1991).

[20] B. S. Ryden and M. Gramann, Astrophys. J. **383**, L33 (1991).

[21] J. Soda and Y. Suto, Astrophys. J. **396**, 379 (1992).

[22] B. Jain and E. Bertschinger, Astrophys. J. **509**, 517 (1998).

[23] L.-Y. Chiang and P. Coles, Mon. Not. R. Astron. Soc. **311,** 809 (2000).

[24] P. Coles and L.-Y. Chiang, Nature (London) **406,** 376 (2000).

[25] L.-Y. Chiang, Mon. Not. R. Astron. Soc. **325,** 405 (2001).

[26] P. Watts, P. Coles, and A. Melott, Astrophys. J. **589,** L61 (2003).

[27] L.-Y. Chiang, P. Naselsky, and P. Coles, Astrophys. J. **602,** L1 (2004).

[28] L.-Y. Chiang, P. Coles, and P. Naselsky, Mon. Not. R. Astron. Soc. **337,** 488 (2002).

[29] P. Coles, P. Dineen, J. Earl, and D. Wright, Mon. Not. R. Astron. Soc. **350,** 989 (2004).

[30] T. Matsubara, Astrophys. J. **591,** L79 (2003).

[31] C. Hikage, T. Matsubara, and Y. Suto, Astrophys. J. **600,** 553 (2004).

[32] C. Hikage, T. Matsubara, Y. Suto, C. Park, A. S. Szalay, and J. Brinkmann, Publ. Astron. Soc. Jpn. **57,** 709 (2005).

[33] R. M. Szepietowski, D. J. Bacon, J. P. Dietrich, M. Busha, R. Wechsler, and P. Melchior, Mon. Not. R. Astron. Soc. **440,** 2191 (2014).

[34] A. Eggemeier and R. E. Smith, Mon. Not. R. Astron. Soc. **466,** 2496 (2017).

[35] J. Byun, A. Eggemeier, D. Regan, D. Seery, and R. E. Smith, Mon. Not. R. Astron. Soc. **471,** 1581 (2017).

[36] K. Ali, D. Obreschkow, C. Howlett, C. Bonvin, C. Llinares, F. O. Franco, and C. Power, Mon. Not. R. Astron. Soc. **479,** 2743 (2018).

[37] A. Eggemeier, T. Battefeld, R. E. Smith, and J. Niemeyer, Mon. Not. R. Astron. Soc. **453,** 797 (2015).

[38] A. Taruya, T. Nishimichi, and S. Saito, Phys. Rev. D **82,** 063522 (2010).

[39] I. Hashimoto, Y. Rasera, and A. Taruya, Phys. Rev. D **96,** 043526 (2017).

[40] J. Yoo, A. L. Fitzpatrick, and M. Zaldarriaga, Phys. Rev. D **80,** 083514 (2009).

[41] C. Bonvin and R. Durrer, Phys. Rev. D **84,** 063505 (2011).

[42] A. Challinor and A. Lewis, Phys. Rev. D **84,** 043516 (2011).

[43] P. McDonald and A. Roy, J. Cosmol. Astropart. Phys. 08 (2009) 020.

[44] J. T. Nielsen and R. Durrer, J. Cosmol. Astropart. Phys. 03 (2017) 010.

[45] D. Bertacca, R. Maartens, and C. Clarkson, J. Cosmol. Astropart. Phys. 09 (2014) 037.

[46] J. Yoo and M. Zaldarriaga, Phys. Rev. D **90,** 023513 (2014).

[47] E. Di Dio, R. Durrer, G. Marozzi, and F. Montanari, J. Cosmol. Astropart. Phys. 12 (2014) 017; 06 (2015) E01.

[48] F. Bernardeau, S. Colombi, E. Gaztanaga, and R. Scoccimarro, Phys. Rep. **367,** 1 (2002).

[49] F. Bernardeau and P. Brax, J. Cosmol. Astropart. Phys. 06 (2011) 019.

[50] Y.-S. Song, A. Taruya, and A. Oka, J. Cosmol. Astropart. Phys. 08 (2015) 007.

[51] R. J. Scherrer and E. Bertschinger, Astrophys. J. **381,** 349 (1991).

[52] R. Juszkiewicz, D. H. Weinberg, P. Amsterdamski, M. Chodorowski, and F. Bouchet, Astrophys. J. **442,** 39 (1995).

[53] F. Bernardeau and L. Kofman, Astrophys. J. **443,** 479 (1995).

[54] P. A. R. Ade *et al.* (Planck Collaboration), Astron. Astrophys. **594,** A13 (2016).

[55] L. Samushia *et al.*, Mon. Not. R. Astron. Soc. **439,** 3504 (2014).

[56] H. Gil-Marìn, J. Norena, L. Verde, W. J. Percival, C. Wagner, M. Manera, and D. P. Schneider, Mon. Not. R. Astron. Soc. **451,** 539 (2015).

[57] J. Gleyzes, D. Langlois, M. Mancarella, and F. Vernizzi, J. Cosmol. Astropart. Phys. 02 (2016) 056.

[58] D. Alonso, E. Bellini, P. G. Ferreira, and M. Zumalacárregui, Phys. Rev. D **95,** 063502 (2017).

[59] J. S. Y. Leung and Z. Huang, Int. J. Mod. Phys. D **26,** 1750070 (2017).